A Doctoral Dissertation

A study on the physiological mechanism to induce neurodevelopmental dysfunction and cognitive decline of pups by prenatal exposure to high cortisol in rats

Hye-Ji Kim

Department of Medicine

Graduate School

Jeju National University

February 2023

흰쥐에서 태중 고농도의 코티졸 노출이 새끼 쥐의 신경발달장애성 인지 기능 저하를 유발하는 생리학적 기전 규명

지도교수 정 성 철

김 혜 지

이 논문을 의학 박사학위 논문으로 제출함

2023 년 2 월

김혜지의 의학 박사학위 논문을 인준함

심사위원장_____

위　　원_____

위　　원_____

위　　원_____

위　　원_____

제주대학교 대학원

2023 년 2 월

A study on the physiological mechanism to induce neurodevelopmental dysfunction and cognitive decline of pups by prenatal exposure to high cortisol in rats

Hye-Ji Kim

(Supervised by Professor Sung-Cherl Jung)

A thesis submitted in partial fulfillment of the requirement for the degree of doctor of philosophy in medicine

2023.02

This thesis has been examined and approved.

.....

.....

.....

.....

.....

.....

Date

Department of Medicine

Graduate School

Jeju National University

ABSTRACT

The high level of blood cortisol is one of key factors to identify major depressive disorder as well as attention deficit hyperactivity disorder (ADHD) that may be mediated by the dysregulation of brain-derived neurotrophic factor (BNDF) signaling during brain development. As ADHD is a developmental neuropsychiatric disorder, it is possible that cortisol directly affects the cellular signaling involved in neuronal growth and brain development. However, it remains unclear whether and how elevation in cortisol levels during the prenatal period affects brain functions and induces psychiatric disorders. I have previously reported that rat pups (Corti.Pups) born from rat mothers repetitively injected with corticosterone (20 mg/kg/day) during pregnancy exhibited increased plasma cortisol levels, deficits in spatial cognitive functions, and ADHD-like behaviors during the post-weaning period. In this study, I aimed to investigate the cellular mechanisms underlying cognitive dysfunction caused by neurodevelopmental impairments induced by prenatal exposure to high cortisol levels. For this purpose, I performed behavioral experiments to test learning and memory functions in juvenile rat pups, electrophysiological studies to evaluate synaptic functions and cell physiology studies to measure the expressions of neurodevelopment-associated proteins. Behavioral assessments of juvenile Corti.Pups using the Morris water maze and Open field tests suggested a possibility that their spatial learning and memory functions were neurophysiologically downregulated, compared with normal rat pups (Nor.Pups). In the electrophysiological experiments to test membrane excitability and synaptic plasticity in hippocampal CA1 neurons of Corti.Pups (postnatal 13 ~ 18 days) using acute slice patch clamping, the synaptic responses to generate

excitatory postsynaptic currents were remarkably suppressed in Corti.Pups. Furthermore, impairments in synaptic long-term potentiation in CA1 neurons, which is the cellular mechanism to reflect the learning and memory formation, were observed in Corti.Pups. This memory impairment was attributed to the remodeling of synaptic NMDA receptor subunits by the augmentation of synaptic NR2B-mediated responses. These results provide evidence that maternal cortisol imbalances and neuroendocrine dysregulation during pregnancy may directly impair synaptic functions in their pups. Further, enzyme-linked immunosorbent assay revealed a significant reduction in BDNF levels in the prefrontal cortex (PFC) and hippocampus (HPC) of Corti.Pups, compared to that in Nor.Pups. In Western blot experiments, the expression level of PSD-95 was significantly lower in both brain areas of Corti.Pups. Interestingly, mTOR and PKA, which are well-established regulators of BDNF levels, were only less expressed in PFC of Corti.Pups. These results indicate that cortisol potently downregulates developmental signaling in the brain during prenatal and postnatal periods. This suggests that cortisol targets neuroendocrine regulation involving catecholamines, such as dopamine, which is a key factor initiating BDNF-mediated signaling cascades for brain development. Here, I provide experimental evidence demonstrating that compared to Nor.Pups, Corti.Pups exhibit synaptic loss and deficits in hippocampal neurons and those major cellular factors that contribute to neuronal development in the PFC and HPC were significantly less expressed. This study clearly provides evidence that cortisol downregulates synaptic development and functions to be important for learning and memory by triggering neuroendocrine dysregulation during brain development, which may contribute to ADHD pathogenesis.

Keywords : Cortisol, ADHD, Learning and memory, LTP, BDNF, NMDA receptor

CONTENTS

LIST OF ABBREVIATIONS

ADHD	Attention deficit hyperactivity disorder
AMPAR	α-Amino-3-hydroxy-5-methyl-4-isoxazole propionic acid receptor
AP	Action potential
ASD	Autism spectrum disorder
BDNF	Brain-derived neurotrophic factor
cAMP	Cyclic adenosine monophosphate
CREB	cAMP response element-binding protein
CUMS	Chronic unpredictable mild stress
D1R	Dopamine D1 receptor
ELISA	Enzyme- linked immunosorbent assay
EPM	Elevated plus maze
EPSC	Excitatory postsynaptic current
FS	Forced swimming
GPCR	G protein-coupled receptor
HC	Healthy control

HPA	Hypothalamic-pituitary-adrenal
HPC	Hippocampus
LTP	Long-term potentiation
MD	Major depression
MDD	Major depressive disorder
mTOR	Mammalian target of rapamycin
MWM	Morris water maze
NMDAR	N-methyl-D-aspartate receptor
OF	Open field
PFC	Prefrontal cortex
PKA	Protein kinase A
PPF	Paired pulse facilitation
PSD-95	Postsynaptic density protein 95
PTSD	Post-traumatic stress disorder
R_{in}	Membrane input resistance
Rph3A	Rabphilin3A
RMP	Resting membrane potential
SD	Sprague-Dawley

SIB	Self-injurious behavior
trkB	tyrosine receptor kinase B
WC	Whole cell capacitance

LIST OF FIGURES

LIST OF TABLES

1. INTRODUCTION

Cortisol, which is frequently referred as the ‘stress hormone’, is secreted by the adrenal cortex of the kidneys and its secretion is regulated by adrenocorticotropic hormone from the pituitary gland. Cortisol promotes cardiorespiratory activities in a defense mechanism against stress, helping people to act more agile and faster and to make clearer decision by increasing blood sugar. However, excessive secretion of cortisol induced by chronic stress seriously increases blood sugar and blood pressure and weakens the immune system, accelerating aging and disease pathogenesis. Therefore, cortisol levels are commonly used as a major biomarker to determine stress-induced neuropsychiatric disorders. In human studies, it was reported that the serum concentrations of cortisol were higher in patients with major depressive disorder (MDD) than in normal adults and that both serum cortisol and Hamilton Depression Rating Scale were significantly recovered by treatment with the antidepressant, fluoxetine [1, 2]. Particularly, in a previous report to examine the relationship between chronic stress to induce depression and hair cortisol levels in adults, hair cortisol levels were increased in accordance with the increment of depressive responses to stress [3]. These findings suggest that the high cortisol levels are dominantly correlated with depressive symptoms in humans. In an animal study using female rhesus macaques to investigate the correlation between stress and cortisol hypersecretion, chronic stress increased depressive behaviors as well as hair cortisol levels [4].

Although several clinical and animal studies have demonstrated a direct relationship between stress-induced cortisol elevation and neuropsychiatric disorders, other studies have reported inconsistent findings, whereby executive functions did not significantly differ according to

cortisol levels between major depression (MD) and healthy control (HC) groups when performing a prefrontal cortex (PFC) / cingulate-mediated executive functioning task (i.e. Stroop test). However, the MD group exhibited impairments of verbal memory in a hippocampal/mediotemporal-mediated verbal memory task (i.e. Paragraph Recall test) [5]. Therefore, further studies are required to determine whether the elevation of cortisol levels is attributable to stress-induced MDD or results from dysfunction in neuroendocrine systems during MDD induction.

There are also previous results to suggest evidence that cortisol levels are significantly correlated with other neuropsychiatric disorders. The serum levels of cortisol in male children with autism spectrum disorder (ASD) were significantly higher than those in the HC group. Furthermore, in ASD groups, hair cortisol levels increased gradually according to the severity of self-injurious behavior (SIB), compared to those in children not exhibiting SIB [6, 7]. In contrast, compared to patients with MDD, patients with post-traumatic stress disorder (PTSD) and panic disorder exhibited lower levels of hair cortisol and neuroendocrine dysregulation, and abnormal cortisol responses were also observed in patients with anxiety disorder and schizophrenia [8-10]. These studies suggest that cortisol is directly or indirectly related to up- or downregulation of the neuroendocrine system in various neuropsychiatric diseases. Based on these findings, additional studies are required to identify if dysfunction of the neuroendocrine system as well as dysregulation of cortisol secretion are sufficient and/or necessary to trigger the pathogenesis of neuropsychiatric diseases. I have previously reported that prenatal exposure to high cortisol induced attention deficit hyperactivity disorder (ADHD)-like symptoms in behavioral patterns of young rats. The behavioral patterns were evaluated using forced swimming (FS), open field (OF), elevated plus maze (EPM) and Morris water maze (MWM) tests during the immediate post-weaning period. This analysis revealed obvious similarities with behavioral symptoms which are

generally observed in animal models of ADHD, characterized by hyperactivity, impulsivity, impairments in learning and memory functions and inattention [11, 12]. In this regard, a clinical study investigated the cortisol-mediated correlation between offspring and their parents. In that study, authors demonstrated that in late adolescence, cortisol levels were higher in offspring of parents with bipolar disorder (BD) than in offspring of healthy parents, indicating that elevated cortisol levels may be a useful biomarker for identifying vulnerability to affective disorders [13]. Although excessive secretion of cortisol and neuroendocrine dysfunction are frequently implicated in the pathogenesis of stress-induced MDD, clinical trials attempting to downregulate cortisol levels seemed to be ineffective at reducing depressive symptoms in patients [14, 15]. This indicates that neuroendocrine dysregulation in the hypothalamic-pituitary-adrenal (HPA) axis, but not absolute levels of cortisol, may be a key factor underlying MDD induction.

Animal studies have also focused on the importance of neuroendocrine regulation in neuropsychiatric disorders. Stress-induced depression has been reported to result in downregulation of tyrosine receptor kinase B (TrkB) and glucocorticoid receptors, which regulate neuronal structure, function, and hormonal stress responses in PFC and hippocampus (HPC) in male rodents [16, 17]. Furthermore, the expression levels of brain-derived neurotrophic factor (BDNF), postsynaptic density protein 95 (PSD-95) and synaptophysin were significantly reduced in depressive animal models exhibiting increased corticosterone levels [18]. Dysregulation of the neuroendocrine system, which is frequently observed in chronic stress-induced depression, can be reversed by antidepressants in an animal model of depressions. A previous study demonstrated that an antidepressant, *Adansonia digitata L.*, dose-dependently not only reversed weight loss, but also decreased depressive behaviors and plasma cortisol levels. Also this antidepressant dramatically increased BDNF levels under chronic unpredictable mild stress (CUMS)-induced depression [19]. These results strongly suggest that antidepressants may

be effective for reversing neuroendocrine dysregulation and depressive behaviors. In the other study, levo-stepholidine (l-SPD), a specific dopamine D1 receptor (D1R) agonist, activated the adenylyl cyclase (AC) / cyclic adenosine monophosphate (cAMP) / protein kinase A (PKA) signaling cascade and increased the phosphorylation of mammalian target of rapamycin (mTOR) via the PKA/mTOR signaling pathway. This promoted expression of synaptogenesis-related proteins, such as PSD-95, synapsin I and GluR1 in the PFC of a Sprague-Dawley (SD) rat CUMS model [20]. These results indicate that synaptic alterations in specific brain loci may be correlated with the interference of neural circuits contributing to negative emotions and cognitive impairments. Therefore, there is a possibility that high cortisol-induced downregulation of neurotransmitters and abnormal behavioral patterns may contribute to the incomplete neurodevelopment in PFC and HPC, as previously reviewed [21].

Clinical studies examining gender differences in responses to stress protocols have demonstrated that compared to men, women exhibited higher cortisol responses and expression of the BDNF Val66Met polymorphism. These findings indicate that gender-specific mechanisms may exist in women. In fact, prenatal stress-mediated effects from mothers are more likely to be biologically transmitted to their children [4, 11, 22-26]. Nevertheless, it still remains unclear whether and how maternal stress-induced dysregulation of cortisol secretion and neuroendocrine function contribute to neurodevelopmental dysfunction and neuropsychiatric disorders in children. Furthermore, the mechanistic relationship between maternal cortisol and ADHD-like behaviors of offspring and correlation between neurodevelopmental dysfunction and neuroendocrine dysregulation should to be elucidated [11].

Therefore, the present study aimed to identify the cellular mechanisms by which prenatal exposure to high cortisol affects brain development and neuroendocrine systems underlying behavioral and cognitive functions in rat pups and to elucidate the pathogenic mechanisms of

ADHD. To this end, I hired cell-physiological, electrophysiological, and behavioral methods, using a rat model.

2. MATERIALS AND METHODS

Animals

SD rats used in this experiment were bred in the animal facility of the Medical School of Jeju National University. The environment of the breeding room was automatically controlled at a temperature of 23 ± 3℃ and humidity of 50 ± 10%. The lighting system was set to repetitively turn on and off for 12 hours a day. Food and water were provided ad libitum. One female rat and one male SD rat were mated in a cage for breeding. All animal experiments and procedures were performed with approval from the Animal Care and Use Committee of Jeju National University.

Drug treatment

Corticosterone (Sigma, St. Louis, MO, USA) was dissolved in normal saline (0.1% Tween 80; Sigma, 0.9% NaCl; Sigma, in DW). Right after confirming the successful mating, 7 ~ 8-week-old pregnant rats were subcutaneously injected with corticosterone (20 mg/kg) or normal saline (as control) daily for 21 consecutive days until delivery (Fig. 1).

Table 1. Exposure to high cortisol during pregnancy reduces offspring weight.

	p1	p7	p14	No. of Pups
Nor.Pup	7.74 ± 0.19	21.10 ± 0.91	41.90 ± 1.65	10.00 ± 0.71
Corti.Pup	6.03 ± 0.15 **	17.27 ±0.53 **	31.40 ± 0.89 **	10.33 ± 1.51 NS

Data indicate the mean ± S.E. **, $p < 0.01$, compared with Nor.Pups. NS, not significant.

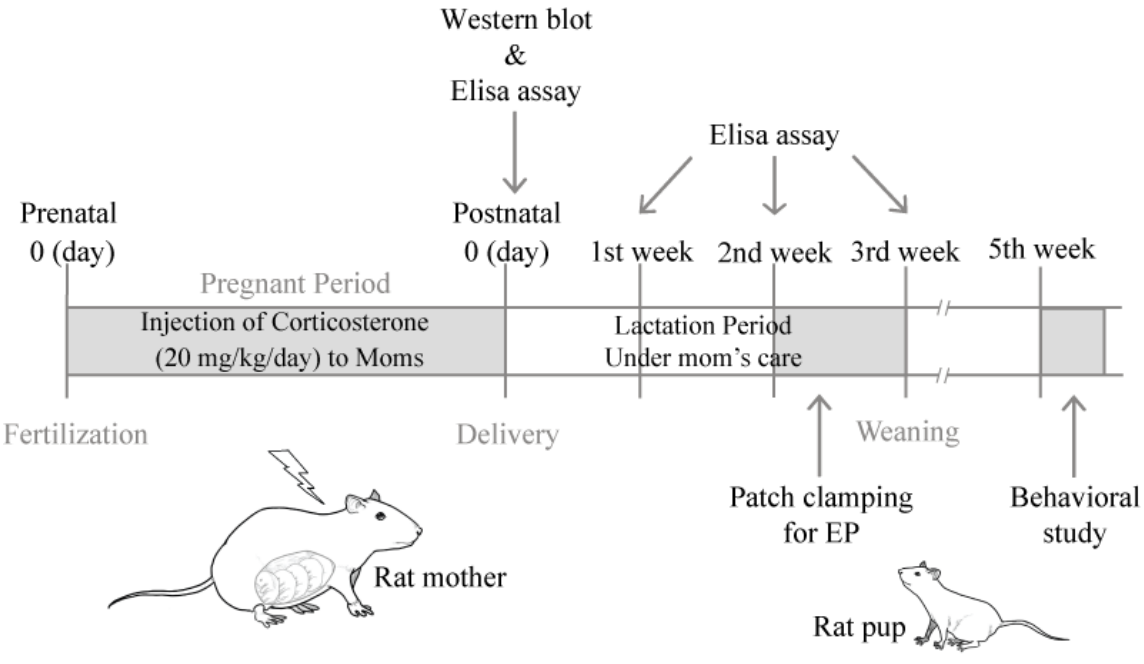

Figure 1. Experimental scheme of the rat model.

Behavioral experiments

Behavioral experiments involving male and female pups were performed from postnatal day 35 to day 40. MWM and OF tests were conducted between 9:00 ~ 11:00 AM and 1:00 ~ 5:00 PM, respectively. All rat pups were transferred to the testing room 30 min before the trial to habituate to experimental conditions of air temperature 22 ~ 24℃. The test room was soundproof, and the light intensity was set at 200 ~ 250 lux with overhead LED fluorescent lamps (20 watt). All behaviors and locomotor activities of pups were recorded using action cameras (AS30 of Sony and Yi of Xiaomi) and tracked for analysis using idTracker software (Ver. 4.97, idtracker.es/home).

Morris water maze (MWM) test

Spatial cognitive function of rat pups was measured using the MWM test. The MWM test was conducted using a metal cylinder chamber with 120 cm in diameter and 50 cm in depth. The tank was filled with water suspended in non-toxic white paint to submerge a platform made of transparent plexiglass. The water temperature was set to 24.0 ± 1℃. The water height was sufficiently deep such that rats were unable to touch the bottom. The hidden square platform (400 cm^2) was submerged 1 ~ 2 cm below the surface in the center of the north quadrant. The second test was performed 10 minutes after the first test, and the final experiment was performed 24 hours later to evaluate short and long term-memory functions. Swimming activities were monitored via an action camera mounted overhead, and recorded for analyzing via a tracking program. All rat pups were allowed 300 seconds to find the hidden platform and tests were immediately finished if rat pups found and stayed on the hidden platform for over 5 seconds. The swimming latency and distance to reach the platform, and the spent time in the target quadrant were analyzed and compared with each other group.

Open field (OF) test

Spontaneous locomotor activity was measured using the OF test. The OF box comprised a cube without a ceiling (80 cm × 80 cm and height of 50 cm), which was constructed of white PVC fomex (5 mm thickness). The bottom of the open cube was divided into 16 small squares using 3 horizontal and vertical lines and four small squares located in the center were defined as the center area. The room temperature was set at 22 ~ 24℃. The test was performed once daily from postnatal days 38 ~ 41 to 42 ~ 45. Rat pups were allowed to move freely in the box for 5 minutes in each test, and after each test session, the OF box was cleaned thoroughly with a 70% ethanol solution to remove the scent of previous test animals. Behavioral patterns of rat pups in the OF test were evaluated by measuring the total travel distance, central travel distance, center-to-total distance ratio, and movement velocity.

Tissue preparation for patch-clamping

Acute hippocampal slices were prepared from SD rat pups on the postnatal days 13 ~ 18. The rats were decapitated under ether anesthesia, and the brains were immediately removed, hemisected and placed in 0 ~ 4℃ cutting solution containing (in mM): 125 NaCl, 2.5 KCl, 25 $NaHCO_3$, 1.25 NaH_2PO_4, 25 glucose, 0.5 $CaCl_2$ and 5 $MgCl_2$ (pH 7.25). Sagittal slices (350 μm) were made using a vibratome (LEICA VT100S). During the preparation of acute slices, the cutting solution was saturated by bubbling with 95% O_2 and 5% CO_2 for over 10 minutes. The slices were transferred to normal recording solution containing artificial cerebrospinal fluid (ACSF–external solution) and incubated at 35℃ for 10 min. The recording solution contained (in mM): 125 NaCl, 2.5 KCl, 25 $NaHCO_3$, 1.25 NaH_2PO_4, 25 glucose, 2 $CaCl_2$, and 1 $MgCl_2$ (pH 7.4). 5 μM 2-chloroadenosine was added for all recordings. All recordings were performed at room temperature.

Electrophysiology

Acute hippocampal slices were transferred to a submerged recording chamber with a continuous flow of the recording solution (continuously bubbled with 95% O_2 and 5% CO_2) for whole-cell patch-clamp recordings. The slices were visualized using a BX50 microscope (Olympus, Japan) through a 40X water-immersed objective. Patch electrodes with 4–6 MΩ tip resistances were pulled using a PP-830 (Narishige, Japan) and then filled with the internal solution containing (in mM): 20 KCl, 125 K-gluconate, 10 HEPES, 4 NaCl, 0.5 EGTA, 4 ATP, 0.3 TrisGTP, and 10 Phosphocreatin (pH 7.2, 290–320 mOsm). All electrophysiological recordings were performed using a HEKA patch system (EPC9/2), and data acquisition and analysis were performed using Pulse (HEKA, Germany) and IGOR Pro (Wavemetrics, Lake Oswego, Oswego, USA) softwares.

Synaptic long-term potentiation (LTP) of hippocampal CA1 neurons was induced by a pairing protocol, which consisted of low frequency stimulation (4 Hz) paired with membrane depolarization to 0 mV for 1 min. The synaptic responses were evaluated by measuring excitatory postsynaptic current (EPSC)s that were triggered by repetitive stimulations (0.1 Hz) applied to the Schaffer collateral (SC) pathway, and the synaptic potentiation was analyzed by measuring EPSC amplitudes for 10 minutes before and 30 minutes after LTP induction.

To electrophysiologically measure and separate postsynaptic responses of each glutamate receptor, total EPSCs of CA1 neurons were first measured at -65 mV holding potential in Mg^+-free external recording solution by stimulating SC pathway (0.1 Hz). The intensity of the stimulation was adjusted so that EPSC amplitudes were approximately 100 pA. After recording total EPSCs for 5 minutes, DNQX (15 μM), a α-amino-3-hydroxy-5-methyl-4-isoxazole propionic acid receptor (AMPAR) blocker, was added to Mg^+-free external recording solution to

isolate N-methyl-D-aspartate receptor (NMDAR)-mediated EPSCs. After confirming the effect of DNQX by observing the complete blockade of AMPAR-mediated EPSCs (approximately 10 min after application), putative NR2A subunit-mediated EPSCs were acquired by adding ifenprodil (3 μM), which is known to block NR2B-mediated EPSCs, to the Mg^{+}-free external solution containing DNQX. NR2A-mediated EPSCs were recorded for 20 min after washing under 'DNQX + ifenprodil' and then, the remained EPSCs were finally blocked by adding APV (10 μM) during the last 5 min for confirming that those were NR2A-mediated EPSCs.

For observing subthreshold and suprathreshold excitabilities of hippocampal CA1 neurons, various current pulses were injected through recording pipettes under a current-clamp mode. Current pulses applied to change membrane potentials were stepped from −200 pA to 200pA with 50 pA steps and 800 ms duration. Subthreshold excitabilities were monitored by observing membrane input resistance (R_{in}) and voltage sags during hyperpolarization, and suprathreshold excitabilities were determined by measuring the frequencies of repetitive action potential (AP)s at each positive current pulse injection and AP onset times.

Paired pulse facilitation (PPF) and the ratio of EPSC amplitude to stimulation intensity were measured to evaluate the presynaptic and postsynaptic properties during the synaptic transmission between SC pathway and CA1 neurons, respectively. PPF was measured by inducing two EPSCs with 50 msec interstimulus intervals and quantified by averaging with the amplitudes of 10 traces. Therefore, PPF values indicate the ratio of the second stimulus-evoked EPSC peak to the first stimulus-evoked EPSC peak.

Enzyme- linked immunosorbent assay (ELISA)

BDNF levels in the PFC and HPC of rat pups were determined using BDNF Chemikine TM kit (Millipore; CYT306). The assay was performed according to the manufacturer's instructions.

Brain tissues were collected from rat pups on postnatal days 7, 14 and 21. Standard and test samples were incubated overnight at 4℃ in a 96-well precoated dish with an anti-BDNF polyclonal antibody. Standard curves were generated using known amounts of the growth factor. The detection system included a biotinylated anti-BDNF monoclonal antibody with a streptavidin-HRP conjugated solution. The chromogenic substrate solution of tetramethylbenzidine was added to the plate and the reaction was stopped by adding the stop solution provided in the kit. The changed colors induced by the oxidation–reduction reaction were measured using a plate reader set at a wavelength of 450 nm. The standard curve for BDNF provided a linear plot of absorbance versus concentration, which was used to determine BDNF concentration in tissue samples.

cAMP concentrations were measured using the cyclic AMP XP ® Assay Kit (Cell Signaling Technology). Acute PFC and HPC tissues were prepared from rat pups on postnatal day 1. Tissue slices were frozen in liquid nitrogen, and homogenized on ice. cAMP concentrations were determined in 100 μl of each supernatant according to the manufacturer′s instruction and related to the respective protein content of each sample.

Western blot

PFC and HPC tissues were homogenized in ice-cold tissue lysis buffer. Protein extracts were size-separated and electro-transferred onto immuno-blot PVDF membranes. Briefly, the PFC and HPC tissues were separated from brains of rat pups on postnatal day 1 and dissociated by trituration using pipettes and a Dounce-type tissue grinder (Kimble Chase). The clearances of pestle A and B at this stage were 0.0028 ~ 0.0047 mm and 0.0008 ~ 0.0022 mm, respectively. The homogenates were centrifuged at 14,000×g for 30 minutes. All procedures were conducted at 4℃. The isolated proteins were quantified using a Bio-Rad protein assay dye, and the protein

concentration of the lysate was determined using the Lowry protein assay. Protein lysates (30 μg/lane) were resolved on a 10% SDS-PAGE gel, transferred onto PVDF membranes at 250 mA for 75 min, and incubated with anti-mTOR (7C10) Rabbit mAb (1 : 1000, Cell Signaling, USA), anti-PKA alpha polyclonal antibody (1 : 1000, Invitrogen, USA), anti-post synaptic density protein 95 antibody, clone 6G6-1C9 (1 : 1000, Millipore, USA), or anti-β-Actin monoclonal antibody (1 : 5000, Sigma, USA). After washing three times for 5 min with 0.5% TBS-tween, membranes were probed with a secondary antibody anti-rabbit IgG (1 : 5000) and anti-Mouse IgG1 (1 : 5000) for 30 minutes at a room temperature. Finally, membranes were developed using a kit (Thermoscience), and bands were visualized on Medical X-Ray Film blue (AGFA, Mortsel, Belgium). Densitometric analysis was conducted using ImageJ software (NIH, Bethesda, MD, USA).

Statistical analysis

Data analysis was performed using Excel (Microsoft, USA) and SPSS software. All data are presented as mean values ± standard error of mean (SEM). Statistical analysis was performed using a Student's *t*-test and two-way ANOVA, as appropriate. Statistical significance is indicated as p value < 0.05 or < 0.01.

3. RESULTS

To establish the animal model, one 7 ~ 8-week-old female rat and one 8 ~ 9-week-old male rat were mated for 1 week for breeding. Corticosterone (20 mg/kg) was administrated subcutaneously to 7 ~ 8-week-old female rats once daily during pregnancy immediately after confirming fertilization and then rat pups born from them were defined as 'Corti.Pups'. Rat pups born from rat mothers that were treated with saline (0.9% NaCl) or untreated were defined 'Nor.Pups'. Body weight of pups at postnatal 2 weeks was significantly lower in Corti.Pups than in Nor.Pups (Table 1). I have previously reported that Corti.Pups revealed ADHD-like symptoms with delayed cognitive functions in behavioral patterns observed during the post-weaning period [11]. In the present study, I performed cell-physiological and electrophysiological experiments to identify cellular mechanisms whether and how prenatal exposure to high cortisol induced neurodevelopmental and cognitive dysfunctions to affect learning and memory function. I here provide experimental evidence to demonstrate that Corti.Pups have synaptic loss and deficits in functional properties of hippocampal neurons and major cellular regulators contributing to neuronal development in PFC and HPC were significantly less expressed, compared with Nor.Pups. The results are as following.

1. Impairment of long-term memory formation of Corti.Pups was observed in the MWM test during post-weaning period

The MWM test is the most useful to evaluate learning and memory function based on spatial cognitive performance in animal models. Animals are repeatedly placed in a pool of water and forced to escape by finding a hidden platform. Changes of escape latency, moving distance, and

velocity in the MWM water tank are analyzed to estimate learning abilities. The MWM tests were performed using 5-week-old pups in this study. In the first test, pups were subjected to the MWM test for 5 minutes. The second test was performed 10 minutes after the first test and the final test was performed 24 hours after the first test. In the first test, both Nor.Pups and Corti.Pups took a long time and moved a long distance to find the hidden platform, and Corti.Pups showed slightly better performance, with significantly shorter escape time than Nor.Pups (Fig. 2D and 3C, Escape Time, 1st test, Nor.Pup = 141.47 ± 22.67 s, n = 8; Corti.Pup = 94.03 ± 12.81 s, n = 10; $p < 0.05$; Distance, 1st test, Nor.Pup = 29.41 ± 5.02 m, n = 8; Corti.Pup = 20.68 ± 2.84 m, n = 10; n.s). In the second test after 10 minutes, escape time and moving distance of both groups to reach the hidden platform were significantly reduced with no significant differences between two groups, compared with the results of the first test (Fig. 2D and 3C, Escape Time, 2nd test, Nor.Pup = 21.35 ± 4.50 s, n = 8; Corti.Pup = 18.55 ± 3.06 s, n = 10; n.s; Distance, 2nd test, Nor.Pup = 5.05 ± 1.39 m, n = 8; Corti.Pup = 4.19 ± 0.98 m, n = 10; n.s). This result indicated intact short-term memory in spatial cognition in both groups. In the third test executed after 24 hours, Nor.Pups still exhibited significantly shorter escape time and moving distance, similarly to the results of the second test. However, Corti.Pups exhibited significantly longer escape time and moving distance compared to those of the second test, resembling levels of the first test (Fig. 2D and 3C, Escape Time, 3rd test, Nor.Pup = 28.24 ± 4.97 s, n = 8; Corti.Pup = 71.47 ± 17.94 s, n = 10; $p < 0.05$; Distance, 3rd test, Nor.Pup = 5.84 ± 1.33 m, n = 8; Corti.Pup = 16.29 ± 4.40 m, n = 10; $p < 0.05$). These results suggested impaired long-term memory formation in Corti.Pups. Figure 4 presents the average values of normalized time and distance in the second and third tests relative to the results of the first test. Both Nor.Pups and Corti.Pups demonstrated significantly shorter escape time and moving distance in the second test. And then learning and memory functions were maintained in Nor.Pups till 24 hours, but Corti.Pups failed to exhibit complete memory formation in the third test (Fig. 4A,

Time Ratio, 2nd/1st, Nor.Pup = 0.15 ± 0.074, n = 8; Corti.Pup = 0.20 ± 0.045, n = 10; n.s; 3rd/1st, Nor.Pup = 0.20 ± 0.060, n = 8; Corti.Pup = 0.76 ± 0.28, n = 10; $p < 0.05$). This suggests that long-term memory formation after learning tasks was impaired in Corti.Pups.

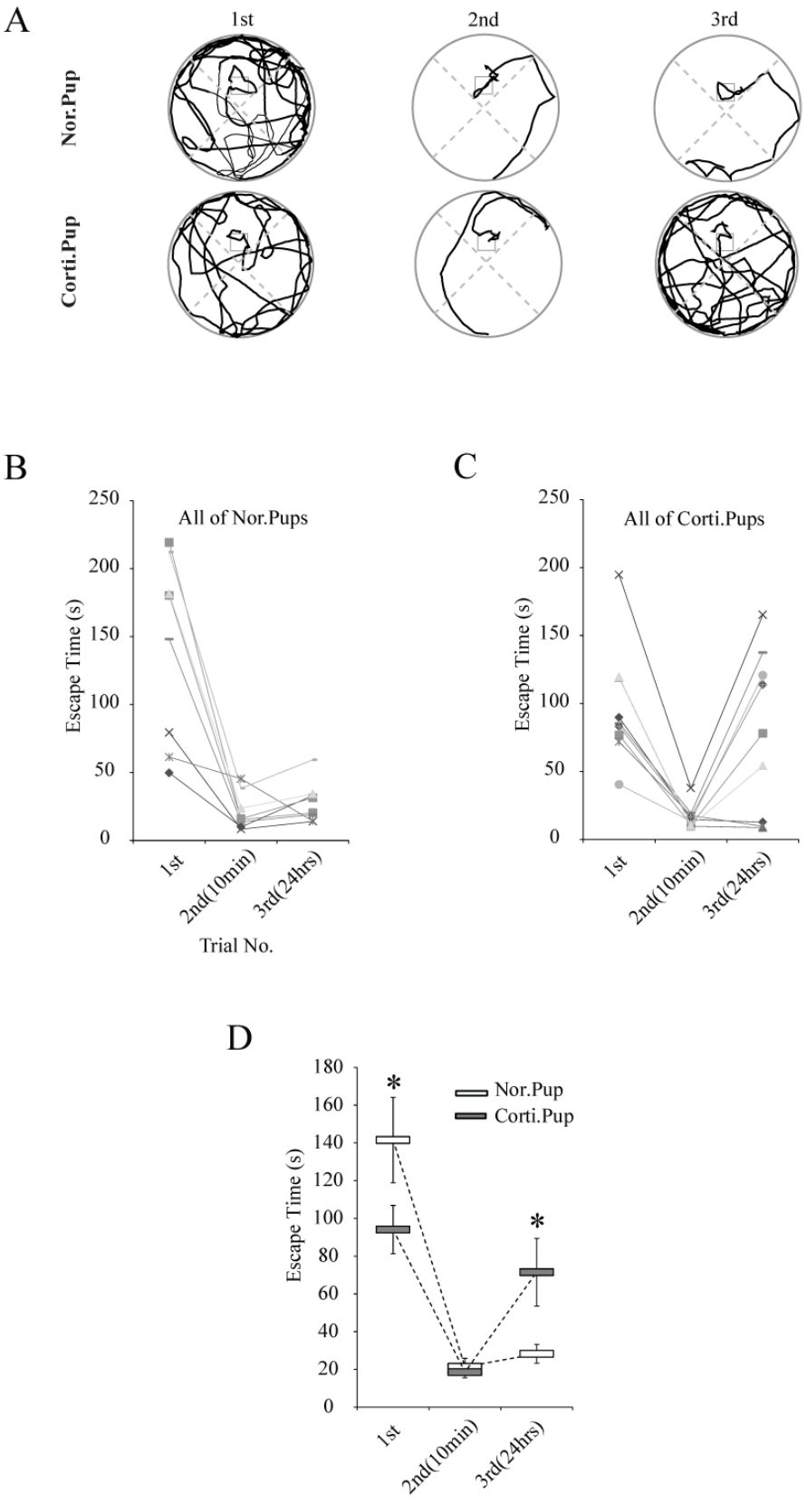

Figure 2. Corti.Pups exhibited longer escape times in the MWM test.

A. Example traces of swimming activities of pups during three MWM tests. The 2nd and 3rd tests were performed 10 minutes and 24 hours after the 1st test, receptively. **B** and **C.** The individual changes of escape time of rat pups. **D.** The averaged values of escape times. Corti.Pups exhibited significantly longer escape time than Nor.Pups in the 3rd test, almost returning to the levels of the 1st test. Data indicate the mean ± S.E. *, $p < 0.05$, compared with each other group.

A

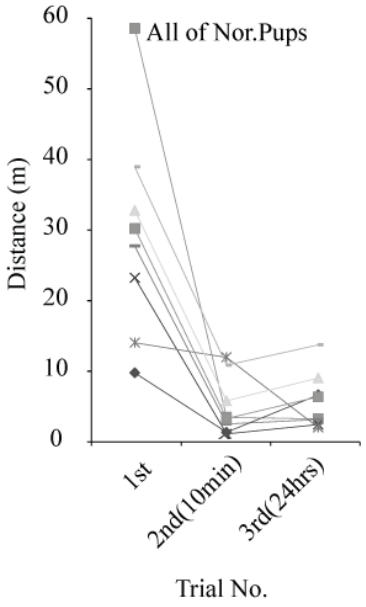

B

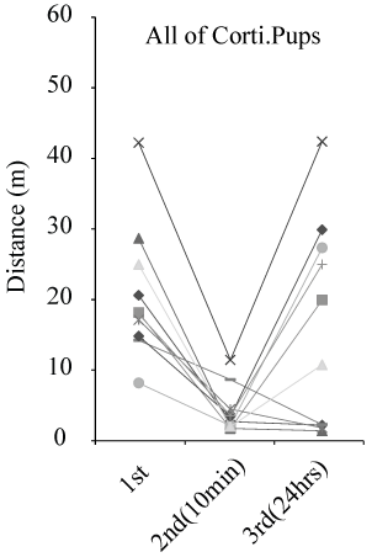

C

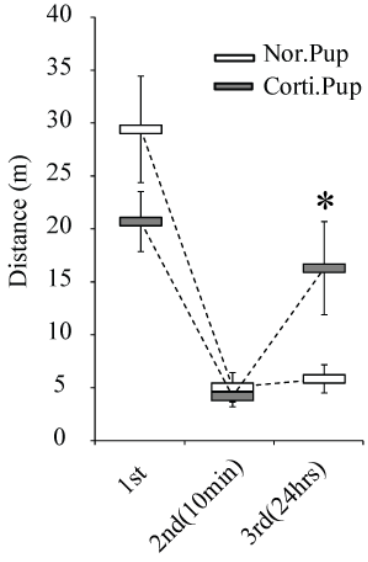

Figure 3. Corti.Pups exhibited longer moving distance in the MWM test.

A and **B.** The individual changes of travel distance of rat pups. **C.** The averaged values of travel distances. Both groups showed similar travel distances in the 1st and 2nd test. However, Corti.Pups required a longer travel distance to find the hidden platform in the 3rd test, showing the incomplete formation of long-term memory. Data indicate the mean ± S.E. *, $p < 0.05$, compared with each other group.

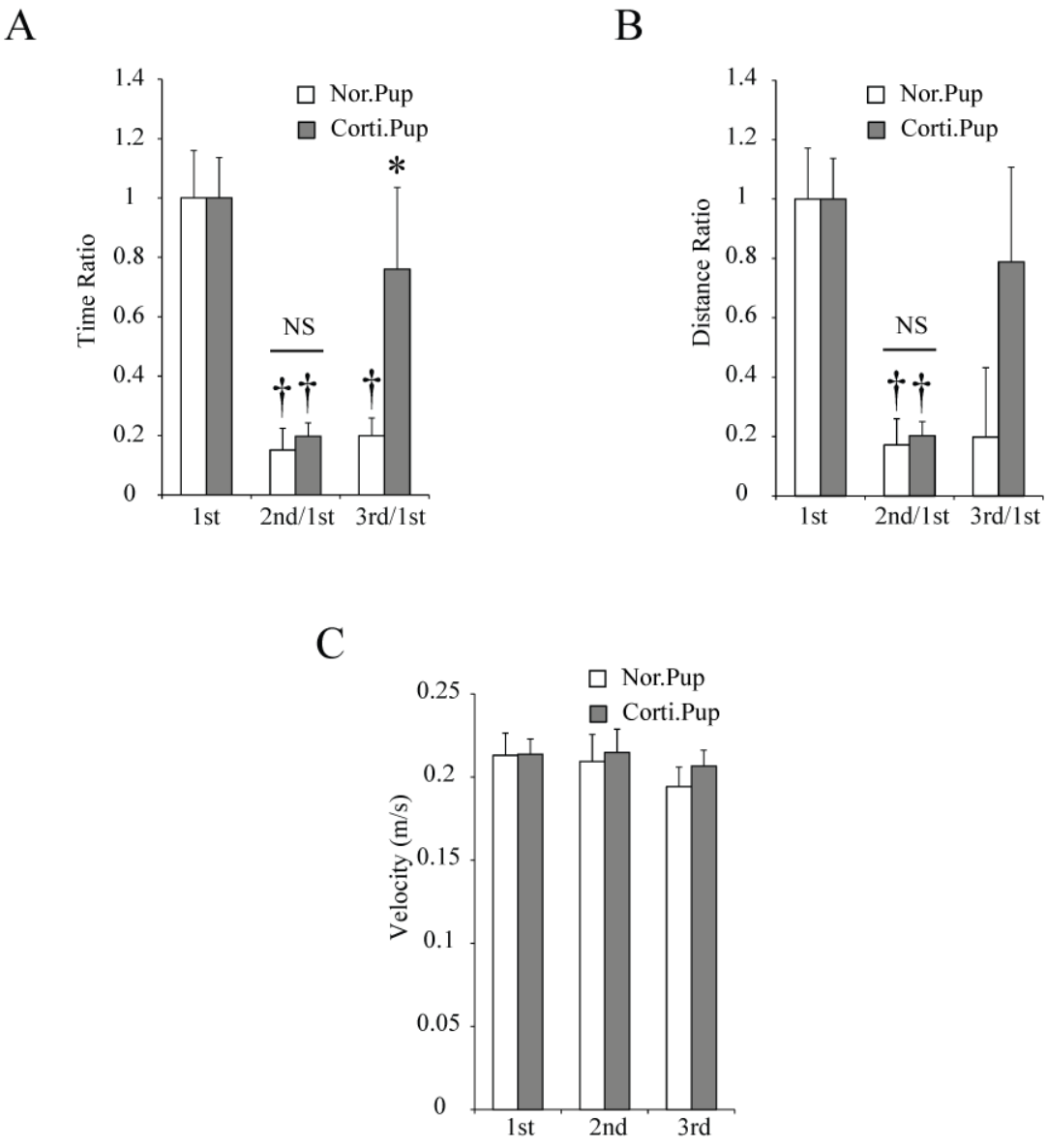

Figure 4. Corti.Pups exhibited the impairment of learning and memory in the MWM tests.

A and **B.** The average values of normalized time and distance of the 2nd and the 3rd tests based on the results of the 1st test. Both of Nor.Pups and Corti.Pups showed significantly shorter escape time and moving distance in the 2nd test. However, only Nor.Pups but not Corti.Pups showed the complete memory formation in the 3rd test. **C.** Averaged swimming velocities of both groups. Data indicate the mean ± S.E. *, $p < 0.05$, compared with Nor.Pups; †, $p < 0.05$, compared with 1st test. NS, not significant.

2. Cognitive impairment in Corti.Pups revealed by behavioral analysis of target quadrant movements

Figure 5 presents a comparison of target quadrant movement and annulus time between the two groups. The target quadrant refers to the center of 45 degree-rotated north quadrant containing the hidden platform, whereas annulus time refers to the time for the rat pups to first step onto the hidden platform. Target quadrant times and travel distances in both groups were significantly lower in the second test than in the first test. However, Corti.Pups exhibited significantly longer time and distance to find and stay in the target quadrant in the third test, compared to the second test (Fig. 5A and B, Target quadrant time, 3rd test, Nor.Pup = 9.47 ± 0.60 s, n = 8; Corti.Pup = 19.22 ± 3.62 s, n = 10; $p < 0.05$; Target quadrant travel distance, 3rd test, Nor.Pup = 1.54 ± 0.17 m, n = 8; Corti.Pup = 3.78 ± 0.86 m, n = 10; $p < 0.05$). These results suggested that Corti.Pups exhibited significantly more untargeted movements compared to Nor.Pups. Moreover, the first annulus time to reach the hidden platform was significantly shorter in Corti.Pups in the first test, and both groups exhibited significantly shorter first annulus time in the second test, with no differences between groups. However, Corti.Pups demonstrated a trend for increased first annulus time in the third test, but this did not reach statistical significance (Fig. 5C, First annulus time, 1st test, Nor.Pup = 129.25 ± 21.97 s, n = 8; Corti.Pup = 67.30 ± 11.43 s, n = 10; $p < 0.05$; 3rd test, Nor.Pup = 22.56 ± 4.93 s, n = 8; Corti.Pup = 52.59 ± 15.22 s, n = 10; n.s). These results implied cognitive abnormalities and more untargeted movements in Corti.Pups regarding spatial memory. For a more detailed analysis, I subtracted quadrant time and first annulus time from escape time to identify the time taken to find the hidden platform in target quadrant area (Fig. 6). In the first test, Corti.Pups exhibited significantly better performances compared to Nor.Pups. In the second test, both groups required significantly shorter times to enter the target quadrant and escape compared to the first test. However, in the

third test, Corti.Pups exhibited significantly longer escape time after entering the target quadrant compared to Nor.Pups (Fig. 6A, Escape time – Quadrant time, 1st test, Nor.Pup = 107.19 ± 18.01 s, n = 8; Corti.Pup = 67.90 ± 9.86 s, n = 10; $p < 0.05$; 3rd test, Nor.Pup = 18.77 ± 4.58 s, n = 8; Corti.Pup = 52.25 ± 14.61 s, n = 10; $p < 0.05$). In Figure 6B, the analysis of 'Escape time – First annulus time' confirmed that Corti.Pups took longer to escape in the third test, even though they quickly reached the hidden platform in the first test (Fig. 6B, Escape time – First annulus time, 1st test, Nor.Pup = 12.22 ± 5.95 s, n = 8; Corti.Pup = 26.73 ± 7.85 s, n = 10; $p < 0.05$; 3rd test, Nor.Pup = 5.67 ± 0.14 s, n = 8; Corti.Pup = 18.89 ± 12.22 s, n = 10; $p < 0.05$). Taken together with the data shown in Figure 2, the behavioral patterns of Corti.Pups implied the deficits in learning and memory with more untargeted movements. These findings are consistent with a previous study reporting ADHD-like behaviors and cognitive delay in Corti.Pups [11].

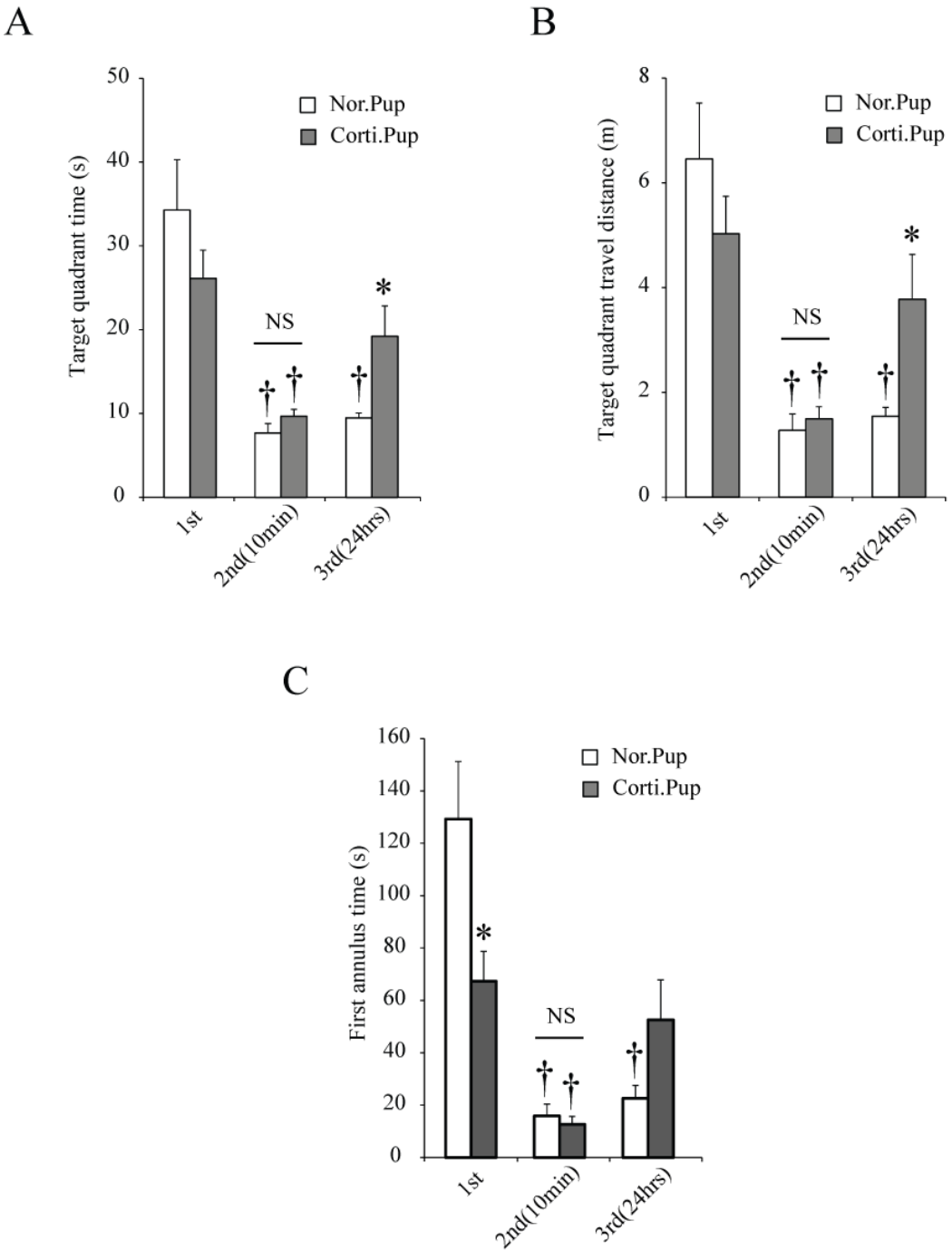

Figure 5. Corti.Pups exhibited increased untargeted movement.

A and **B.** Averaged spent times and travel distances in the target quadrant. Corti.Pups stayed significantly longer in the target quadrant during the 3rd test than Nor.Pups, possibly demonstrating hyperactivities. **C.** Averaged first annulus times of two groups. In the 1st test, the first annulus time to visit the hidden platform was significantly shorter in Corti.Pups than Nor.Pups and both groups showed the reduced first annulus times without any differences in the 2nd test. However, Corti.Pups showed the slightly increased first annulus time in the 3rd test, but not significant between two groups. Data indicate the mean ± S.E. *, $p < 0.05$, compared with Nor.Pups; †, $p < 0.05$, compared with 1st test. NS, not significant.

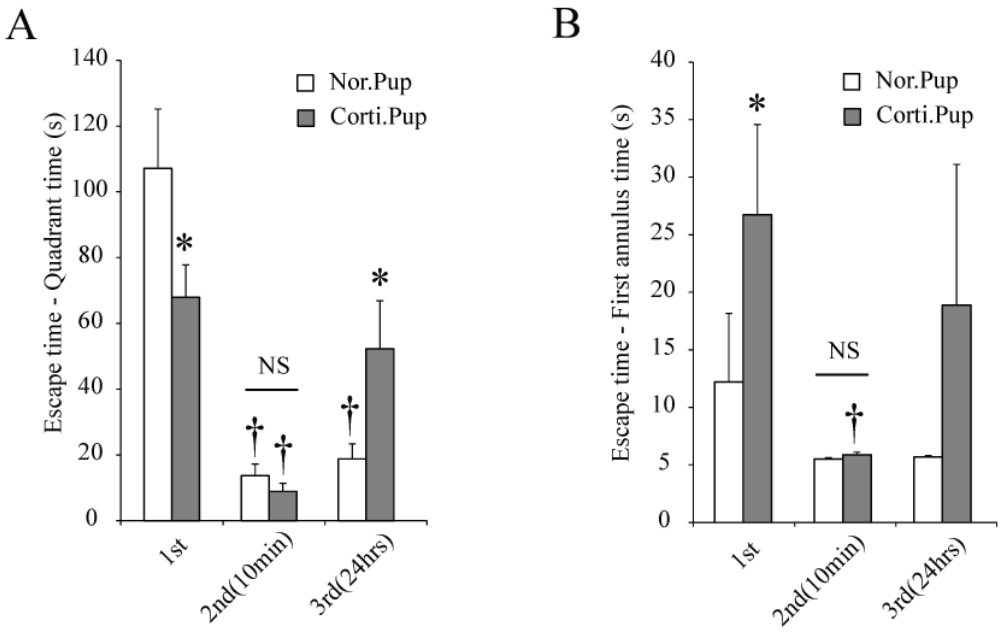

Figure 6. Corti.Pups exhibited cognitive decline in long-term trials in the MWM test.

A. Averaged values of 'Escape time – Quadrant time'. In the 1st test, Corti.Pups exhibited significantly faster performances than Nor.Pups, and in the 2nd test, both groups required significantly shorter times to enter the target quadrant and then escape, compared with the 1st test. However, in the 3rd test, Corti.Pups showed significantly longer escape times after entering the target quadrant than Nor.Pups. **B.** The difference of escape time taken since the first annulus visit. Corti.Pups showed significantly longer escape time despite the first annulus time was significantly shorter in the first test, indicating the possibility of attention deficit. Data indicate the mean ± S.E. *, $p < 0.05$, compared with Nor.Pups; †, $p < 0.05$, compared with the 1st test. NS, not significant.

3. Corti.Pups exhibited hyperactive behaviors in OF test

The OF test is commonly used to measure the ability to adapt to open environments by evaluating behavioral and gross locomotion, and exploratory behavior in rodent models. In this study, I performed the OF test once daily for 3 days and analyzed movements of pups recorded for 5 minutes in each test (Fig. 7). Compared to Nor.Pups, Corti.Pups exhibited significantly longer total moving distance over 3 days, even though the total moving distances in both groups decreased gradually over three days of tests (Fig. 8A, Total distance, day1, Nor.Pup = 30.17 ± 2.84 m, n = 7; Corti.Pup = 38.57 ± 2.36 m, n = 8; $p < 0.05$; day3, Nor.Pup = 14.20 ± 2.79 m, n = 7; Corti.Pup = 24.26 ± 4.14 m, n = 8; $p < 0.05$). Interestingly, Corti.Pups did not exhibit a significant reduction in moving distance in the center field following repeated tests, while Nor.Pups exhibited a significant decrease of center moving distance on the second and third days (Fig. 8B, Center distance, day1, Nor.Pup = 1.73 ± 0.18 m, n = 7; Corti.Pup = 2.59 ± 0.54 m, n = 8; n.s; day2, Nor.Pup = 0.72 ± 0.20 m, n = 7; Corti.Pup = 2.13 ± 0.53 m, n = 8; $p < 0.05$; day3, Nor.Pup = 0.64 ± 0.18 m, n = 7; Corti.Pup = 1.98 ± 0.93 m, n = 8; n.s). Therefore, the ratio of center moving distance to the total moving distance was significantly decreased in the Nor.Pup group but not in the Corti.Pup group was significantly decreased on the second day. As the total moving distance of both groups significantly decreased, the ratio of center moving distance to total moving distance was not reduced on the third day (Fig. 9A, Center distance/total distance * 100, day2, Nor.Pup = 2.64 ± 0.58, n = 7; Corti.Pup = 5.75 ± 1.07, n = 8; $p < 0.05$). In particular, moving velocity was higher in Corti.Pups than in Nor.Pups, indicating that their hyperactivities were being expressed (Fig. 9B, Velocity, day1, Nor.Pup = 0.10 ± 0.0095 m/s, n = 7; Corti.Pup = 0.13 ± 0.0079 m/s, n = 8; $p < 0.05$; day2, Nor.Pup = 0.082 ± 0.0088 m/s, n = 7; Corti.Pup = 0.11 ± 0.0097 m/s, n = 8; $p < 0.05$; day3, Nor.Pup = 0.047 ± 0.0093 m/s, n = 7; Corti.Pup = 0.080 ± 0.014 m/s, n = 8; $p < 0.05$). Overall, Nor.Pups demonstrated instinctive adaptability to the open

environment, which manifested as staying in corners and reduced total movement over repetitive tests. However, Corti.Pups exhibited longer moving distance without a reduction in center area movement, suggesting the expression of hyperactive behaviors as well as the deficits in adaptability.

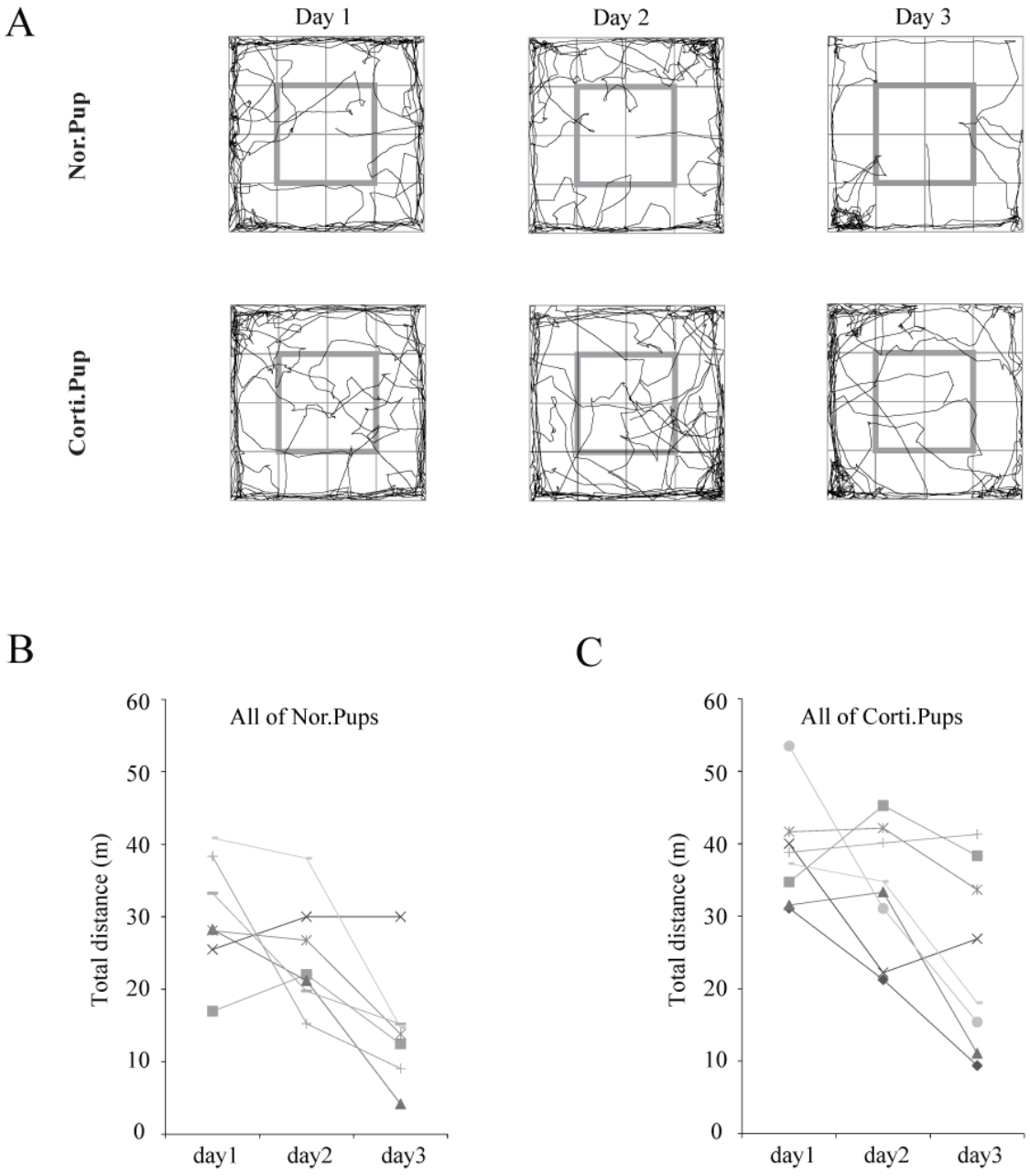

Figure 7. Corti.Pups exhibited longer moving distances in the total and center areas than Nor.Pups in OF test.

A. Example traces of spontaneous movements of rat pups in OF test. **B** and **C.** Individual changes of the total moving distances of rat pups during three OF tests.

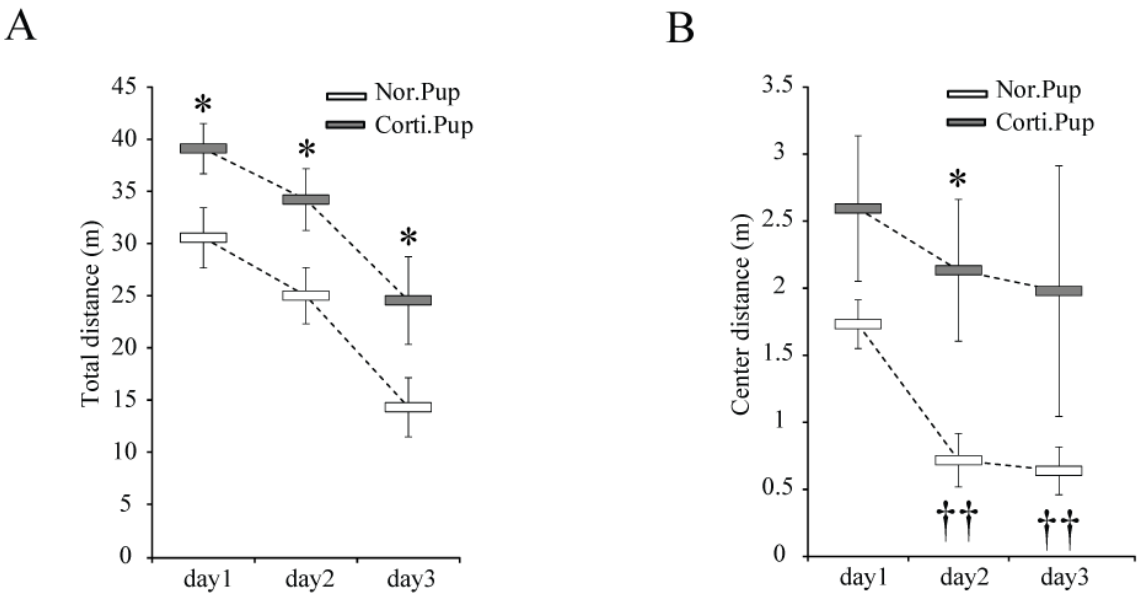

Figure 8. Corti.Pups exhibited no reduction of the center moving distance over three OF tests.

A. Averaged changes of the total moving distances during three OF tests. Corti.Pups showed significantly longer total moving distances for three days than Nor.Pups. **B.** Averaged changes of moving distances in the center area. Corti.Pups did not show any significant reduction of center moving distances, while the significant decrease was observed in Nor.Pups in the second and third days. Data indicate the mean ± S.E. *, $p < 0.05$, compared with Nor.Pups; ††, $p < 0.01$, compared with the first day.

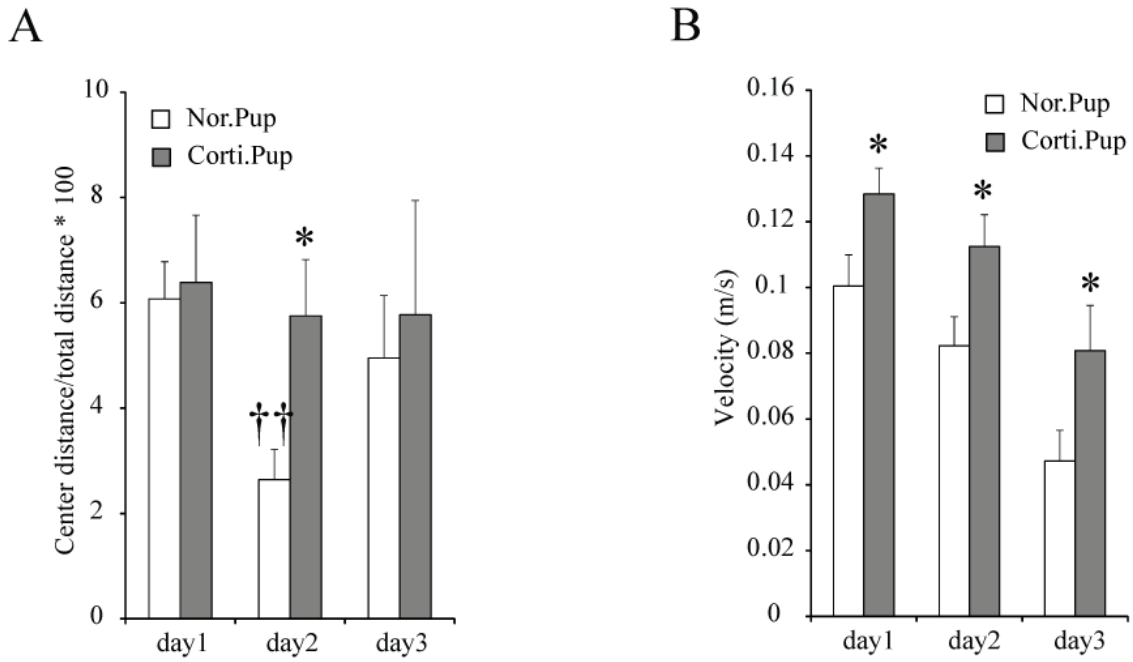

Figure 9. Different patterns of behavioral activities between Nor.Pups and Corti.Pups in OF test.

A. The averaged ratio of center moving distance to the total moving distance. The ratio of center moving distance of Corti.Pups was significantly higher in the second day than that of Nor.Pups. **B.** Averaged changes of moving velocity of pups in OF test. Corti.Pups exerted the faster velocities than Nor.Pups during three OF tests. Data indicate the mean ± S.E. *, $p < 0.05$, compared with Nor.Pups; ††, $p < 0.01$, compared with the first day.

4. Incomplete formation of synaptic LTP was not completely formed in hippocampal CA1 neurons of Corti.Pups

The behavioral patterns of Corti.Pups shown in the MWM test revealed impaired learning and memory functions (Fig. 2 ~ 6). To further investigate the mechanisms underlying these behavioral phenomena at the neuronal level, I examined synaptic plasticity of CA1 neurons, which is a well-established mechanism of memory formation in the mammalian hippocampi. I examined synaptic LTP of EPSCs in hippocampal CA1 neurons using whole-cell voltage-clamp recordings with acute brain slices. The hippocampal slices were acquired from postnatal day 14 ~ 18 Nor.Pups and 13 ~ 18 Corti.Pups. This period is considered to encompass almost complete growth of synaptic structure. I induced NMDAR- and Ca^{2+}-dependent synaptic LTP in CA1 pyramidal neurons by applying a pairing protocol consisting of SC stimulations for 1 minute at 4 Hz with postsynaptic depolarization induced by holding the membrane potential at 0 mV in voltage-clamp mode (Fig. 10A). After applying the pairing protocol to induce LTP, EPSCs were recorded for 30 minutes and their amplitudes were compared between pre- and post-pairing stimulation. In this experiment, Nor.Pups exhibited enhanced EPSC amplitudes, which persisted for 30 minutes. This was the typical synaptic LTP pattern occurring during learning and memory formation in mammalian hippocampi (Fig. 10B and 11). EPSCs recorded in hippocampal CA1 neurons of Corti.Pups also exhibited significantly enhanced amplitude in the early phase after LTP induction. However, the enhancement of EPSC amplitude decreased gradually, and so the potentiation almost completely disappeared in the late phase (Fig. 10B and 11). This indicated that Corti.Pups failed to exhibit complete synaptic LTP in their hippocampi. Figure 12 presents the normalized EPSC amplitudes recorded in the early phase (1 ~ 5 minutes) and late phase (26 ~ 30 minutes) after LTP induction. Corti.Pups demonstrated early potentiation even though their potentiation was less than that of Nor.Pups. However, at the late phase, the potentiation observed

in Corti.Pups had returned to baseline levels, while Nor.Pups exhibited consistent potentiation of EPSCs (Fig. 12, % Change of EPSC amplitude, 1 ~ 5 min, Nor.Pup = 90.49 ± 7.20, n = 7; Corti.Pup = 42.57 ± 4.86, n = 12; $p < 0.01$; 26 ~ 30 min, Nor.Pup = 54.30 ± 3.14, n = 7; Corti.Pup = 5.18 ± 2.23, n = 12; $p < 0.01$). Taken together, these results indicated that synaptic LTP was not properly formed in hippocampal CA1 neurons of Corti.Pups.

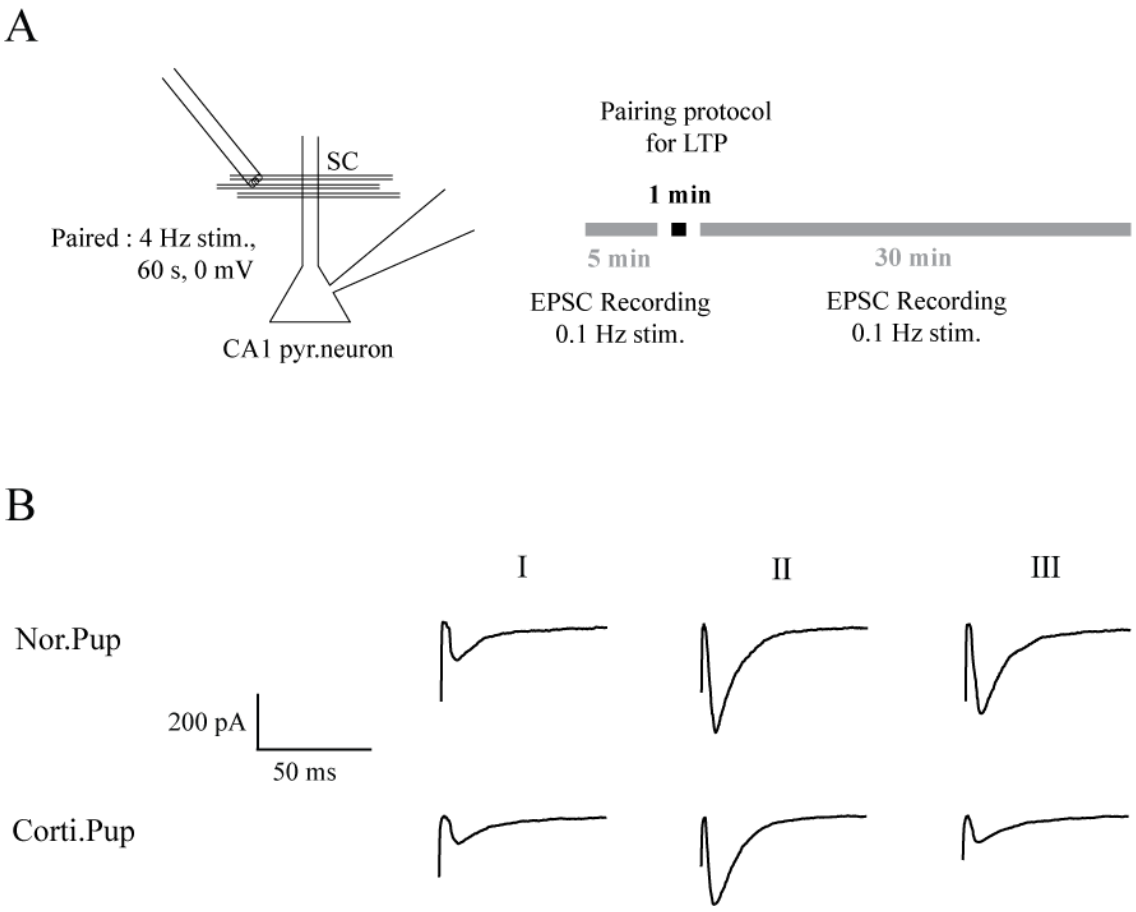

Figure 10. Induction of NMDAR-dependent LTP in Nor.Pups and Corti.Pups.

A. Experimental schema for the conditioning stimulation to induce synaptic potentiation between SC pathway and CA1 neurons. Synaptic LTP was induced by 4 Hz stimulation of the SC pathway for 1 min paired with membrane depolarization at 0 mV holding potential. **B.** Example traces of EPSCs recorded in CA1 neurons before and after LTP induction. The number 'I', 'II', and 'III' are EPSCs recorded before, 1 minute and 28 minutes after LTP induction, respectively, as marked in Figure 11.

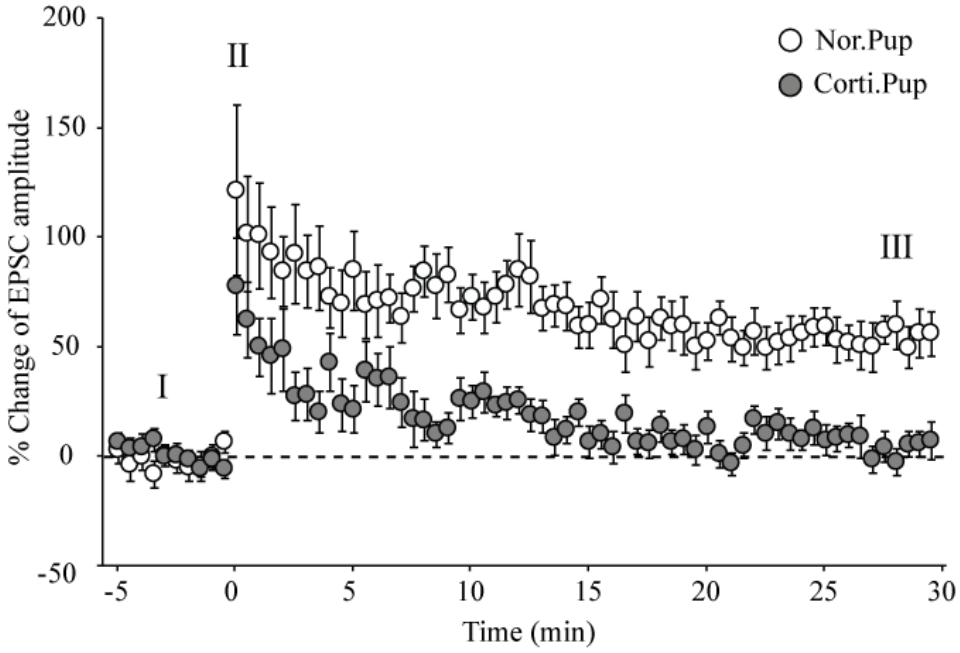

Figure 11. Incomplete LTP was observed in Corti.Pups.

The averaged changes of EPSCs amplitude in hippocampal CA1 neurons before and after applying the pairing protocol to induce LTP (0 minute in X axis). Unlike Nor.Pups, the early potentiation of EPSC amplitude of Corti.Pups was gradually decreased and almost disappeared in the late phase (III).

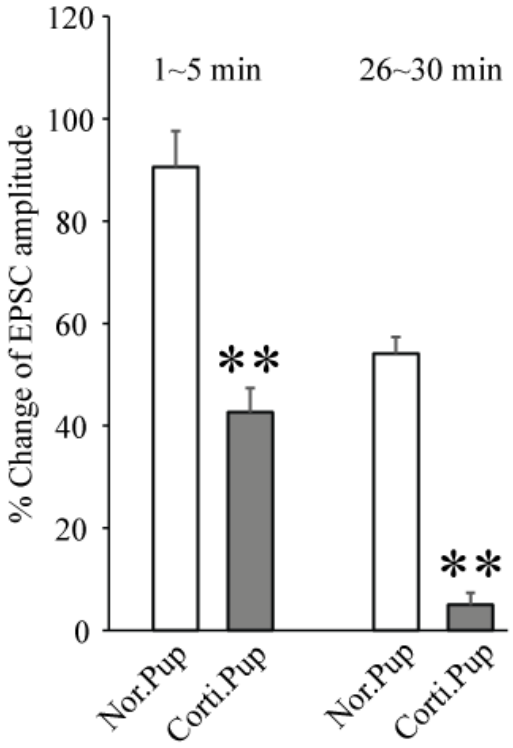

Figure 12. Comparison of potentiation in the early and late phases after LTP induction in CA1 neurons between Nor.Pups and Corti.Pups.

A pairing protocol induced incomplete synaptic LTP in CA1 neurons of Corti.Pups. Both induction and maintenance of LTP were significantly suppressed by the exposure to high cortisol condition during a neonatal period. Data indicate the mean ± S.E. **, $p < 0.01$, compared with each other group.

5. Higher ifenprodil-sensitivity of NMDARs in CA1 neurons of Corti.Pups

As synaptic LTP induced by the pairing protocol is NMDAR-dependent, incomplete LTP induction indicates that the synaptic composition of NMDAR subunits may differ from typical representation during brain development. Therefore, I observed electrophysiologically glutamatergic responses which were required for LTP in CA1 neurons by comparing the functional expression levels of AMPARs and NMDARs. To determine the AMPAR/NMDAR ratio in postsynaptic sites of CA1 neurons, EPSCs were evoked by biphasic electric pulses delivered to SC pathway of the HPC. Total 'AMPAR + NMDAR'-mediated EPSCs were measured in Mg^{2+}-free external solution by opening NMDARs at the resting membrane potential (RMP). Next, pure NMDAR-mediated EPSCs were isolated by adding 15 μM DNQX to block AMPARs. NR2A-mediated EPSCs were measured by adding 3 μM ifenprodil to block NR2B-containing receptors. Subsequently, 50 μM APV was added to the external solution to confirm whether the last EPSCs were mediated by NR2A-containing NMDARs (Fig. 13A). This protocol enable electrophysiological confirmation of the composition of glutamate receptors in postsynaptic CA1 neurons [29]. For this experiment, EPSCs were recorded in hippocampal CA1 neurons of postnatal days 16 ~ 18 in both groups. The Mg^{2+}-free external solution was flowed into the recording chamber containing a brain slice from 10 minutes before recording and EPSCs were measured for 5 minutes at -65 mV holding potential as a control. And then, DNQX was added for 10 minutes during continuous recording of EPSCs. Next, ifenprodil was added for 20 minutes, and finally washed out with external solution containing DNQX and APV for 5 minutes (Fig. 13B). As results, no differences were observed in the total currents between the two groups. Furthermore, isolated NMDAR-mediated EPSCs following the addition of DNQX did not differ between groups. However, after the addition of ifenprodil, EPSC amplitudes were significantly reduced in Corti.Pups compared to that in Nor.Pups. This indicated that in CA1 neurons,

ifenprodil-sensitive receptors containing NR2B subunits were more highly expressed in Corti.Pups than in Nor.Pups (Fig. 13A and B). The AMPAR and NMDAR, which was analyzed by measuring DNQX-sensitive components, were not significantly different between the two groups. However, ifenprodil-sensitivity was significantly higher in Corti.Pups than in Nor.Pups, suggesting that Corti.Pups exhibited a higher expression of NR2B-containing NMDARs in hippocampal CA1 neurons (Fig. 14 A and B, Normalized ratio, AMPAR EPSC, Nor.Pup = 0.59 ± 0.038, n = 10; Corti.Pup = 0.62 ± 0.036, n = 6; n.s; NMDAR EPSC, Nor.Pup = 0.33 ± 0.043, n = 10; Corti.Pup = 0.35 ± 0.036, n = 6; n.s; Ifen. not sensitive, Nor.Pup = 0.66 ± 0.098, n = 10; Corti.Pup = 0.38 ± 0.071, n = 6; $p < 0.05$; Ifen. sensitive, Nor.Pup = 0.34 ± 0.098, n = 10; Corti.Pup = 0.62 ± 0.071, n = 6; $p < 0.05$). These results demonstrated that the switching of NMDAR subunits in postsynaptic sites, which typically occurs during the neurodevelopmental period, was deficient in Corti.Pups.

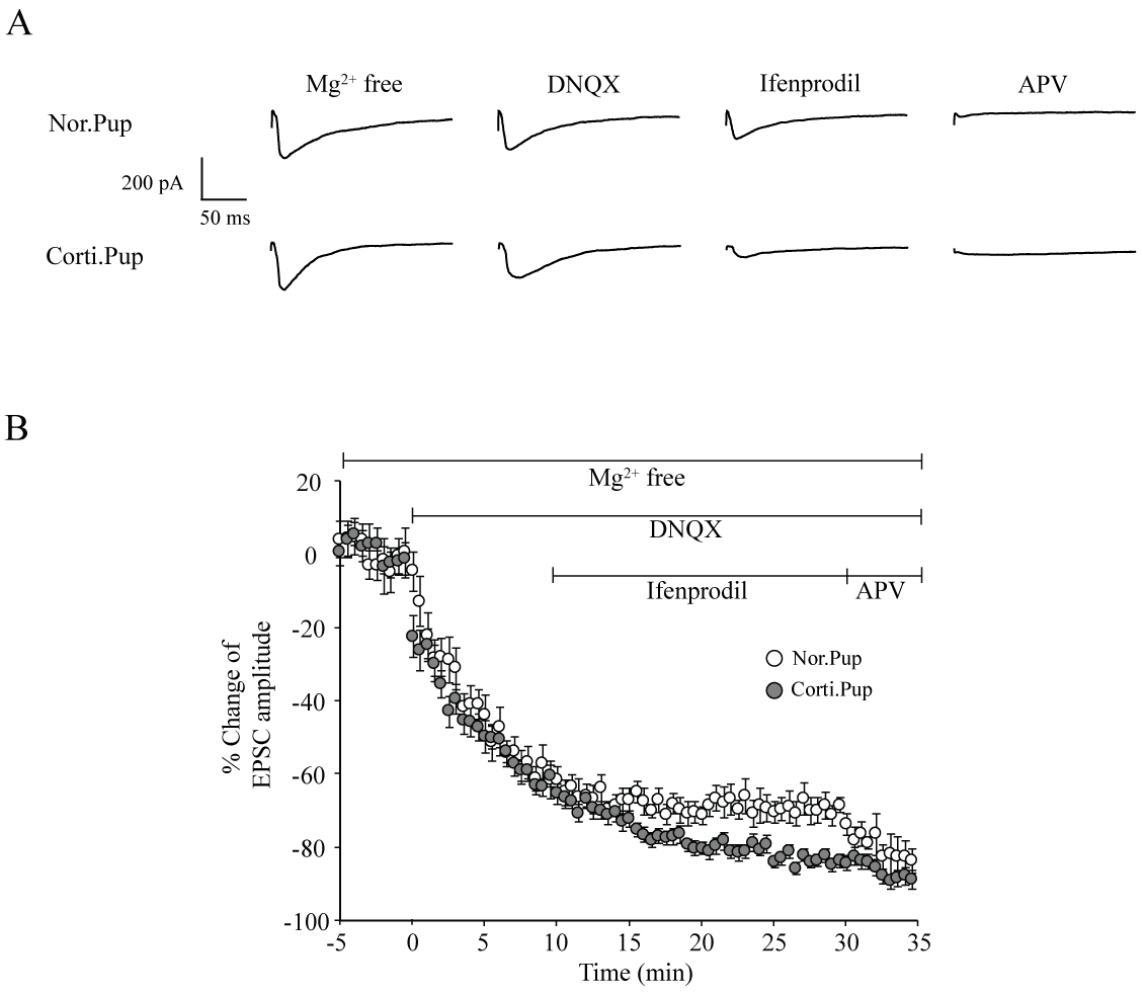

Figure 13. Changes of EPSC amplitude recorded in Mg^{2+}-free external solution.

A. Example traces of EPSCs observed in each condition. **B.** The averaged changes of EPSCs amplitudes during recording. Higher sensitivity to ifenprodil in CA1 neurons of Corti.Pups was observed in this experiment, indicating the different subunit composition of NMDARs or impairment of subunit switching during brain development.

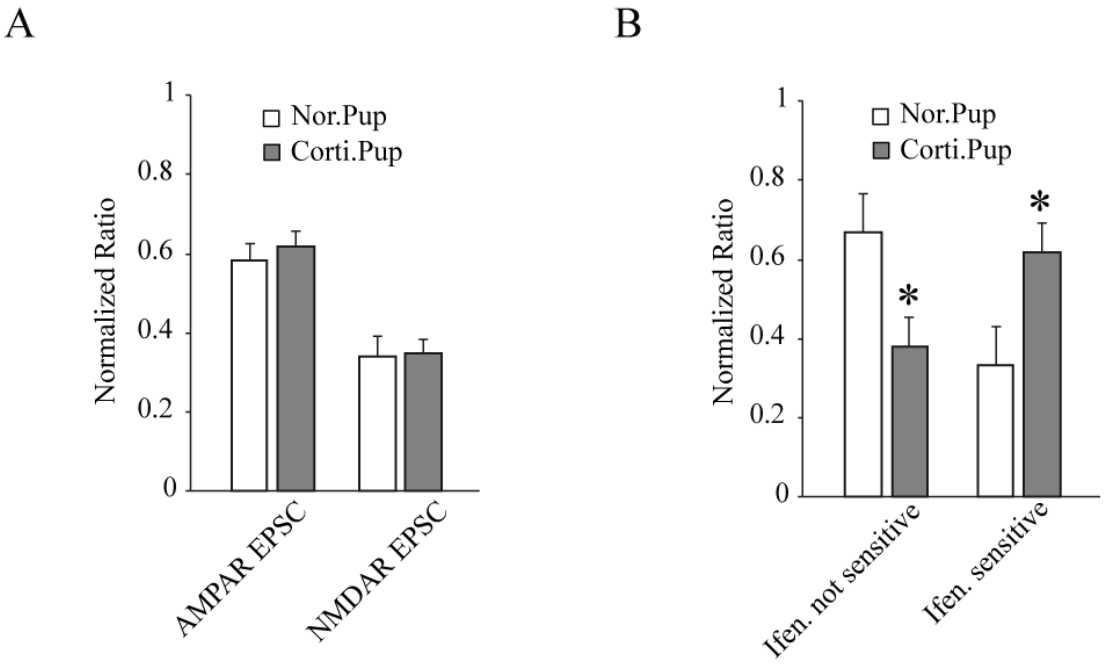

Figure 14. Postsynaptic transmission in Corti.Pups exhibited greater NR2B-mediated responses without any differences in AMPA/NMDA ratio.

A. The averaged ratios of AMPAR and NMDAR EPSCs. There were no differences of EPSC amplitudes of both AMPARs and NMDARs between two groups. **B.** The averaged ratios of ifenprodil-sensitive NMDAR EPSCs. Corti.Pups showed significantly higher sensitivity to ifenprodil in CA1 EPSCs. Data indicate the mean ± S.E. *, $p < 0.05$, compared with each other group.

6. RMP, whole-cell capacitance (WC) and AP threshold of hippocampal CA1 neurons in Nor.Pups and Corti.Pups

As deficient synaptic switching during the early postnatal period indicated neurodevelopmental dysfunction, I next investigated the electrophysiological properties of hippocampal CA1 neurons to compare differences in neuronal properties between Corti.Pups and Nor.Pups using a whole-cell patch clamping. I collected data from hippocampal CA1 neurons of postnatal days 16 ~ 18 pups exhibiting 9 ~ 12 pF of WC, a measurable indicator of cell size, and excluded data that did not fulfill these criteria. Analysis of the correlation between RMP and WC revealed that RMP values of both groups were located within a similar range, but Corti.Pups exhibited a right-biased tendency for WC (Fig. 15), suggesting that the volume of CA1 neurons was larger in Corti.Pups than in Nor.Pups (Fig. 15B, WC, Nor.Pup = 10.67 ± 0.13 pF, n = 23; Corti.Pup = 11.10 ± 0.10 pF, n = 22; $p < 0.01$; RMP, Nor.Pup = -62.61 ± 0.86 mV, n = 23; Corti.Pup = -62.59 ± 1.32 mV, n = 22; n.s). Further, I recorded and compared the threshold of APs in both groups by progressively elevating the membrane potential by applying a lamp current pulse, a protocol that enables accurate measurement AP threshold. AP threshold was slightly but significantly lower in Corti.Pups than in Nor.Pups (Fig. 16A and B, Action potential threshold, Nor.Pup = -45.56 ± 0.84 mV, n = 31; Corti.Pup = -47.67 ± 0.75 mV, n = 26; $p < 0.05$). The significant differences in WC and AP threshold but not in RMP between two groups highlighted different expression levels of membrane proteins affecting neuronal excitability of hippocampal CA1 neurons between Corti.Pups and Nor.Pups.

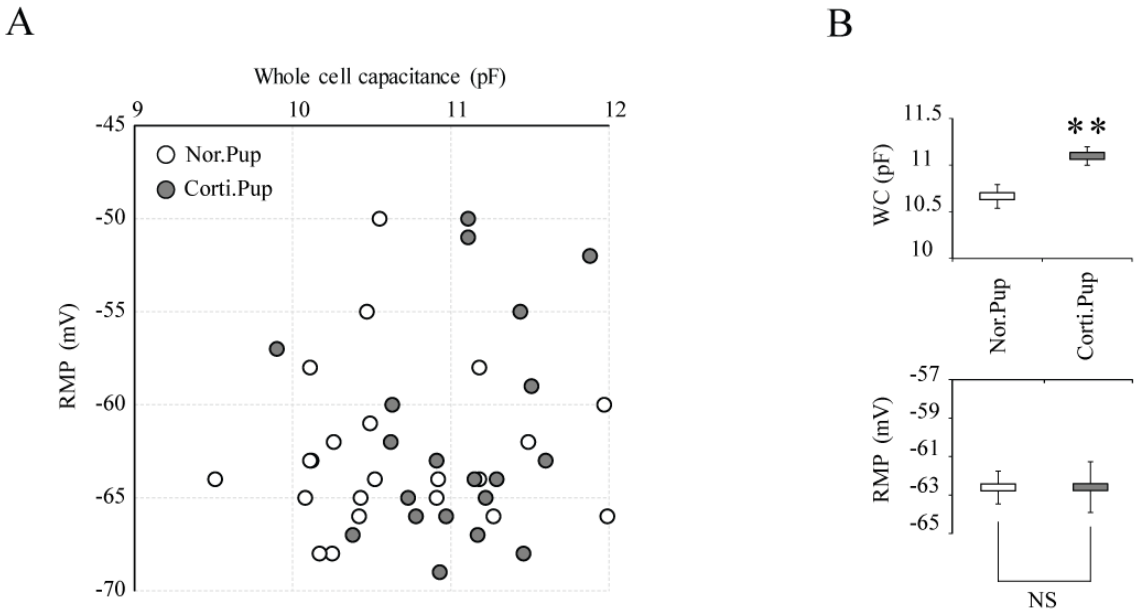

Figure 15. CA1 neurons of Corti.Pups exhibited normal RMP levels and greater WC.

A. The distribution plot of RMP and WC values. Using current-clamping in hippocampal CA1 neurons, RMP and WC were measured and compared between two groups. **B.** The averaged RMP and WC values of two groups. Corti.Pups showed significantly higher WC than Nor.Pups, while no differences were observed in RMP values. This means indicates that Corti.Pups may have different membrane properties in hippocampal CA1 neurons. Data indicate the mean ± S.E. **, $p < 0.01$. NS, not significant.

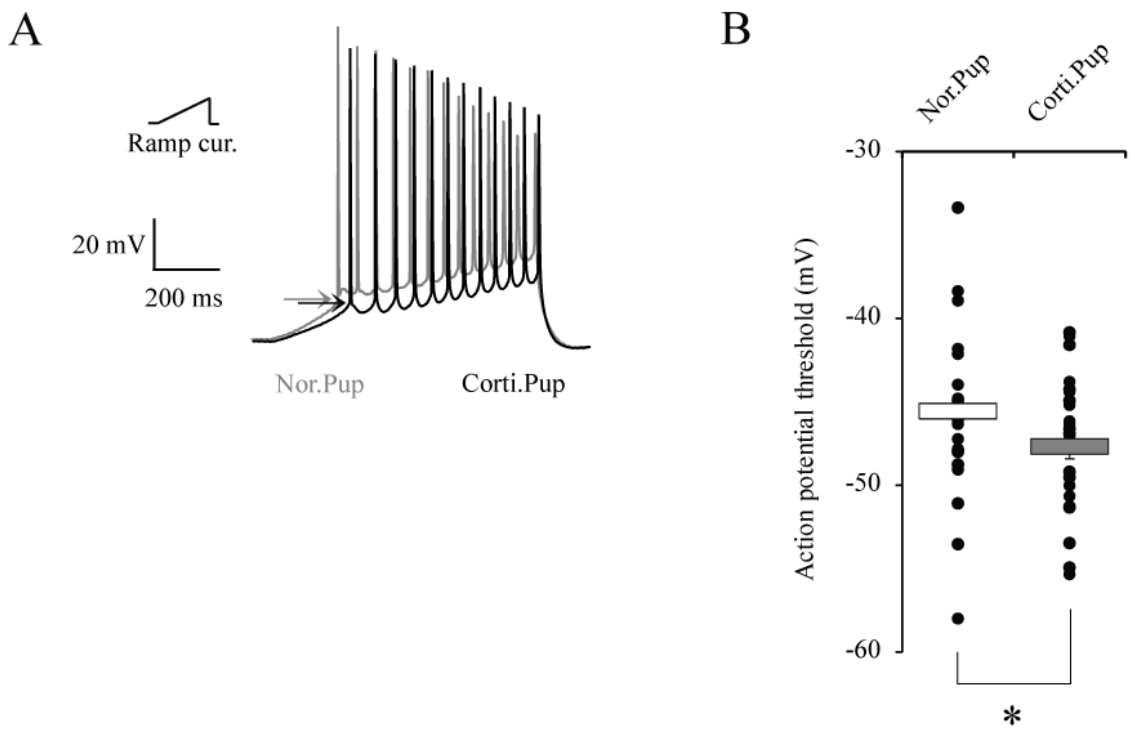

Figure 16. Hippocampal CA1 neurons of Corti.Pups exhibited lower AP threshold.

A. Example traces of APs firing induced by the injection of a ramp current pulse in CA1 neurons, showing the difference of AP threshold between two groups. **B.** Individual and averaged values of AP threshold. Corti.Pups exhibited slightly but significantly lower threshold of APs then Nor.Pups. Data indicate the mean ± S.E. *, $p < 0.05$.

7. Subthreshold and suprathreshold properties of CA1 neurons in rat pups

The current clamping method is an electrophysiological test used to measure the membrane excitability of neurons. This approach provides a useful tool to observe changes in membrane potentials and characteristics of AP firing by applying step-by-step current pulses. The applied current pulse consisted of square current pulses with 50 pA steps ranging from -200 to 200 pA with a duration of 800 ms (Fig 17A and 19A). This protocol commonly enables the analysis of major factors affecting membrane excitabilities of neurons in the subthreshold and suprathreshold ranges. I measured and compared the rate of AP firing and on-set time of APs between the two groups within the suprathreshold range based on RMP levels (Fig. 17 and 18). In levels above 100 pA injections, AP firing rates recorded in CA1 neurons were significantly lower in Corti.Pups than in Nor.Pups (Fig. 17B, Number of action potential/800 ms, 100 pA inj., Nor.Pup = 13.27 ± 0.80, n = 15; Corti.Pup = 10.33 ± 0.85, n = 18; $p < 0.05$; 150 pA inj., Nor.Pup = 18.87 ± 0.75, n = 15; Corti.Pup = 15.94 ± 0.70, n = 18; $p < 0.01$). However, the on-set time of the first AP fired by 100 pA current injection did not show any significant differences between the two groups (Fig. 18B, On-set Time, Nor.Pup = 45.42 ± 13.86 ms, n = 16; Corti.Pup = 36.34 ± 6.45 ms, n = 17; n.s). The lower firing rates of APs observed in Corti.Pups indicated that their hippocampal CA1 neurons might have reduced capacity to fire APs with the given current injections, compared with those in Nor.Pups. The reason underlying the lack of differences in on-set time between the two groups may be due to the differences in WC and AP threshold presented in Figure 15 and 16. Indeed, I observed a lower AP threshold in Corti.Pups suggesting that their neurons were supposed to have shorter on-set time for AP firing. However, the larger WC of Corti.Pups sufficiently delayed AP firing. Based on RMP levels, negative current injections revealed hyperpolarizing properties of neuronal membranes by measuring voltage sags depicting the participation of hyperpolarization-activated cation channels (I_h channels) and by

calculating R_{in} indicating the expression density of cell membrane channel proteins (Fig. 19 and 20). Compared to Nor.Pups, Corti.Pups exhibited significantly smaller voltage sags at the current injection range of -50 ~ -200 pA and their differences were statistically significant. This result suggested significantly lower expression of I_h channels, which prevent membrane hyperpolarization, in Corti.Pups than in Nor.Pups. In particular, these results meant that CA1 neurons of Corti.Pups have poor regulatory functions to adjust membrane excitability, as the expression level of I_h channels is related to the capacity to block membrane hyperpolarization and regulate membrane excitability (Fig. 20A, Voltage sag, -50 pA inj., Nor.Pup = 2.22 ± 0.25 mV, n = 15; Corti.Pup = 1.39 ± 0.19 mV, n = 18; $p < 0.05$; -100 pA inj., Nor.Pup = 5.12 ± 0.51 mV, n = 15; Corti.Pup = 3.04 ± 0.36 mV, n = 18; $p < 0.01$; -150 pA inj., Nor.Pup = 7.42 ± 0.65 mV, n = 15; Corti.Pup = 4.72 ± 0.44 mV, n = 18; $p < 0.01$; -200 pA inj., Nor.Pup = 8.77 ± 0.75 mV, n = 15; Corti.Pup = 5.90 ± 0.52 mV, n = 18; $p < 0.01$) [30]. However, unlike the difference observed in voltage sags, there was no significant difference in R_{in} between Nor.Pups and Corti.Pups (Fig. 20B, R_{in}, -50 pA inj., Nor.Pup = 174.33 ± 17.00 mΩ, n = 15; Corti.Pup = 146.94 ± 10.48 mΩ, n = 18; n.s; -100 pA inj., Nor.Pup = 153.31 ± 13.92 mΩ, n = 15; Corti.Pup = 128.09 ± 7.38 mΩ, n = 18; n.s; -150 pA inj., Nor.Pup = 144.86 ± 12.93 mΩ, n = 15; Corti.Pup = 118.76 ± 5.26 mΩ, n = 18; n.s; -200 pA inj., Nor.Pup = 139.19 ± 12.75 mΩ, n = 15; Corti.Pup = 114.13 ± 5.42 mΩ, n = 18; n.s). This indicates that bilipid membrane properties may also be weakened in Corti.Pups, which exhibit lower expression of membrane proteins.

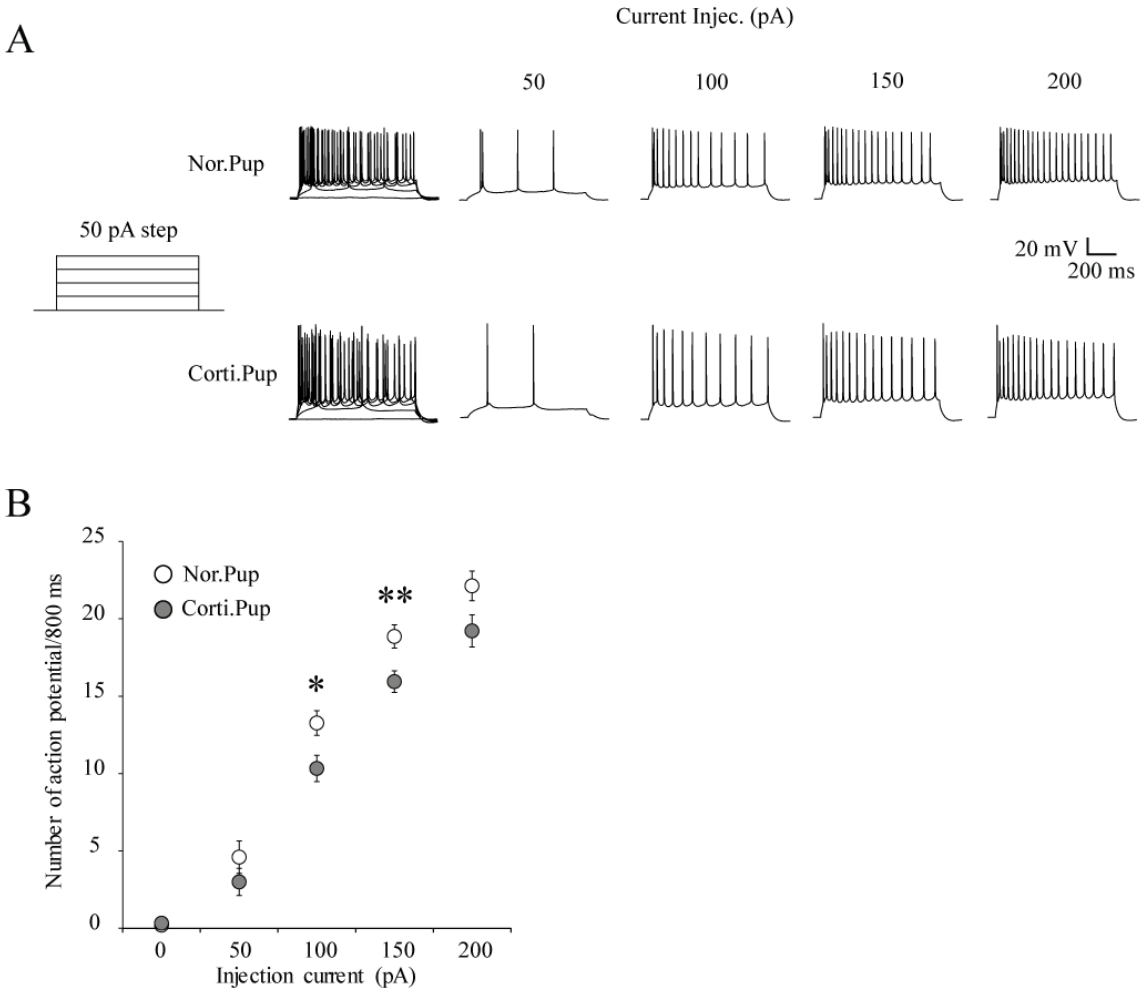

Figure 17. AP firing rates of CA1 neurons observed in the suprathreshold ranges.

A. Example traces of AP firing patterns triggered by positive currents injection of 50 to 200 pA. **B.** The average rates of APs firing in CA1 neurons of two groups. Corti.Pups showed significantly lower firing rates in 100 and 150 pA injections, compared with Nor.Pups. Data indicate the mean ± S.E. *, $p < 0.05$; **, $p < 0.01$, compared with each other group.

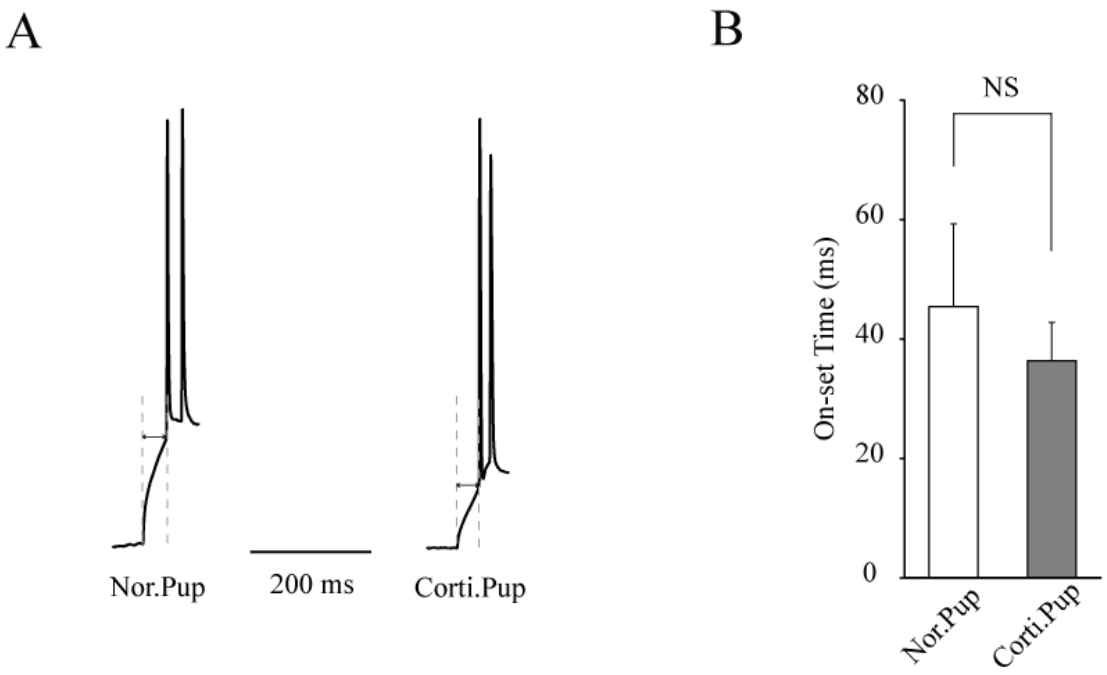

Figure 18. On-set times of APs did not differ significantly between Corti.Pups and Nor.Pups.

A. Example traces to measure the on-set time to the first AP fired by 100 pA current injection. **B.** The averaged values of on-set times. No differences were observed between two groups. NS, not significant.

A

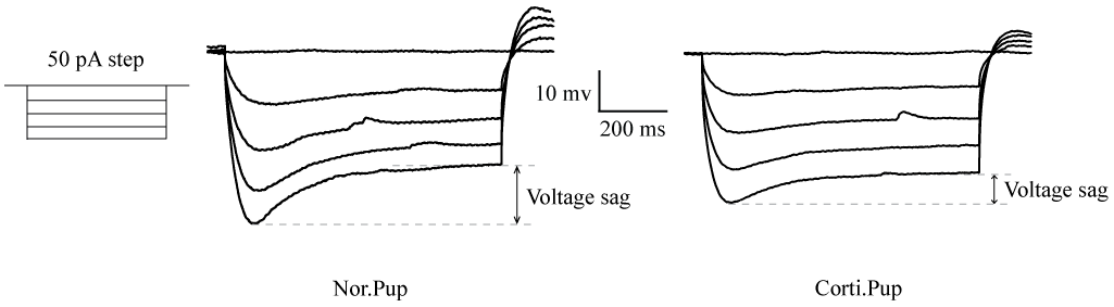

B

$$R_{in} = \frac{\text{Membrane potential late phase (mV)}}{\text{Injected current (pA)}}$$

Figure 19. Voltage sags during membrane hyperpolarization were smaller in Corti.Pups than in Nor.Pups.

A. Example traces of membrane potential changes by injecting negative currents of -50 to -200 pA. **B.** The formula to calculate R_{in} with the changes of membrane potentials by current injections.

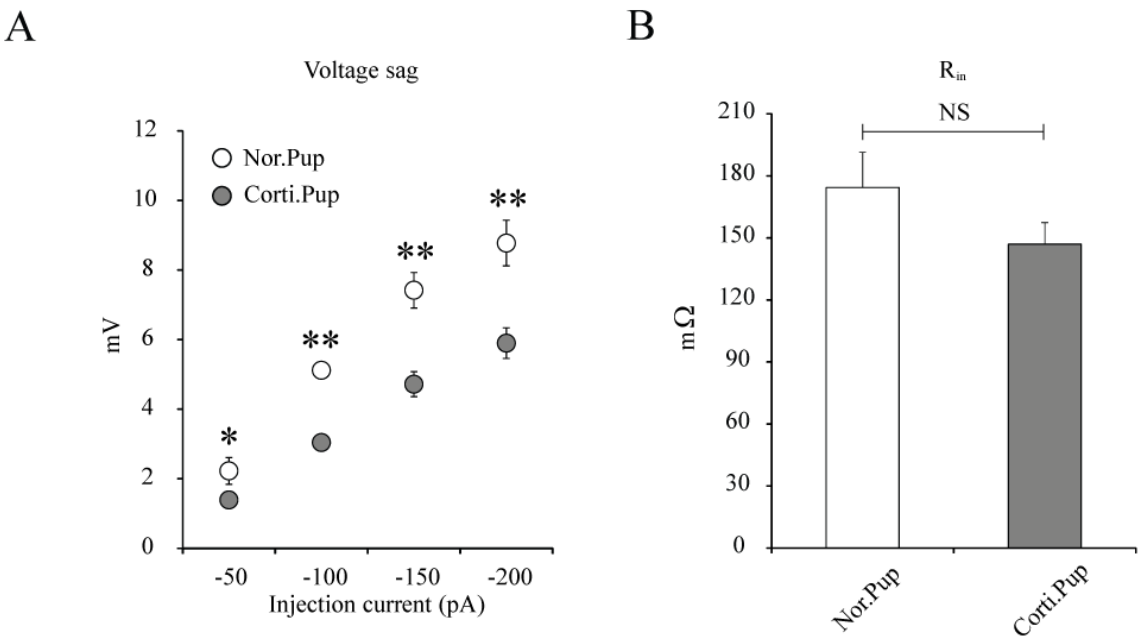

Figure 20. Voltage sags of membrane potential induced by hyperpolarization were significantly smaller in Corti.Pups than in Nor.Pups.

A. Averaged voltage sags. Corti.Pups showed significantly smaller voltage sags at -50 ~ -200 pA ranges of current injections than Nor.Pups. **B.** Averaged R_{in}. There was no statistical significance in different R_{in} between Nor.Pups and Corti.Pups. Data indicate the mean ± S.E. *, $p < 0.05$; **, $p < 0.01$. NS, not significant.

8. Postsynaptic responses but not presynaptic functions of CA1 neurons were weakened in Corti.Pups

My analysis confirmed partial differences in the electrophysiological properties of neuronal membranes of hippocampal CA1 neurons between Nor.Pups and Corti.Pups. Next, the properties of EPSCs, which were evoked by external stimulations applied to the SC pathway, were again observed to evaluate if the presence of distinct characteristics in the synaptic transmission of CA1 neurons, focusing on their presynaptic and postsynaptic functions (Fig. 21 ~ 23). In this experiment, I set artificially the amplitude of EPSCs within 50 ~ 150 pA by adjusting stimulation intensity. Therefore, there were no differences in the amplitude of EPSCs between the two groups (Fig. 21A and 22A, EPSC amplitude, Nor.Pup = 95.84 ± 6.91 pA, n = 13; Corti.Pup = 101.64 ± 6.70 pA, n = 16; n.s). However, quantification of EPSC amplitudes by comparing the correlation with stimulation intensity revealed that significantly stronger stimulations were required to induce EPSCs in Corti.Pups than in Nor.Pups (Fig. 22 B, Stimulation Intensity, Nor.Pup = 0.064 ± 0.0093 mA, n = 13; Corti.Pup = 0.11 ± 0.016 mA, n = 16; $p < 0.05$). This indicated that AMPAR-medicated EPSCs for a given stimulation intensity were weaker in Corti.Pups than in Nor.Pups (Fig. 21B and 22C, EPSC/Intensity Ratio, Nor.Pup = 1.88 ± 0.24, n = 13; Corti.Pup = 1.27 ± 0.19, n = 16; $p < 0.05$). Moreover, this result provided evidence that weak postsynaptic responses to synaptic inputs in Corti.Pups might result in incomplete LTP presented in Figure 10. For evaluating presynaptic activities of CA1 neurons, I measured PPFs of EPSCs, which reflect the capacity for neurotransmitter secretion by inducing the accumulation of neurotransmitters at synaptic cleft with paired stimulations (Fig. 23). PPFs consisted of two EPSCs evoked by applying two consecutive stimuli with an interval of 50 ms, and its ratio was calculated using the difference of amplitudes between the first and second EPSCs. As a result, there was no difference in PPF analysis of EPSCs between the two groups

(Fig. 23B, 2nd stimul., Nor.Pup = 1.70 ± 0.11, n = 8; Corti.Pup = 1.75 ± 0.13, n = 10; n.s). These findings suggest that the weakened synaptic transmission and incomplete LTP pattern observed in Corti.Pups may be attributed to postsynaptic sites and associated functions.

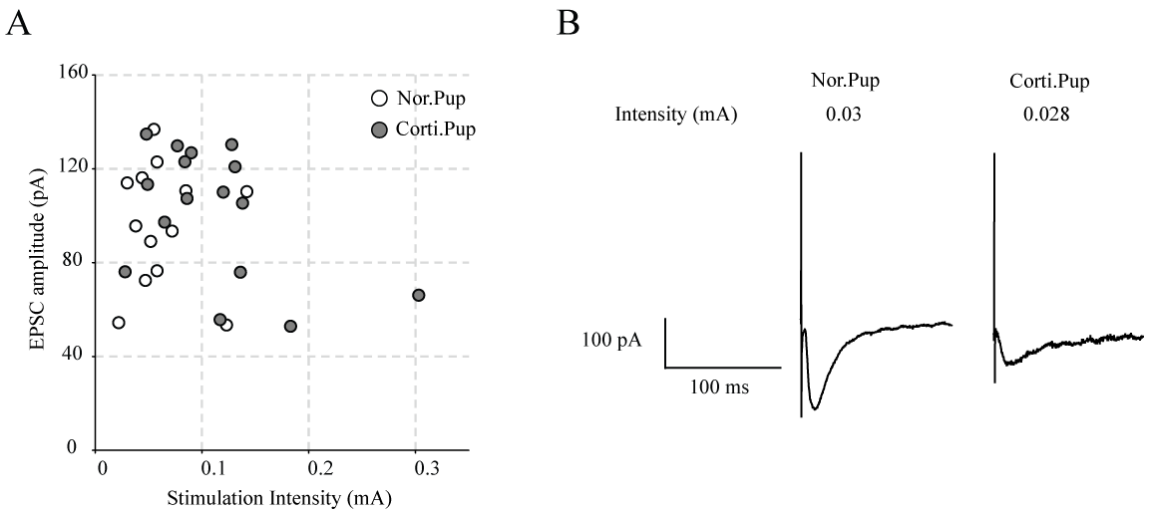

Figure 21. Corti.Pups required stronger stimulation for inducing EPSCs as large as those of Nor.Pups (individual data).

A. The correlation between EPSC amplitude and stimulation intensity in CA1 neurons. **B.** Sample traces of EPSCs evoked by the stimulation with the similar intensity in both groups. Corti.Pups exhibited smaller EPSCs than Nor.Pups.

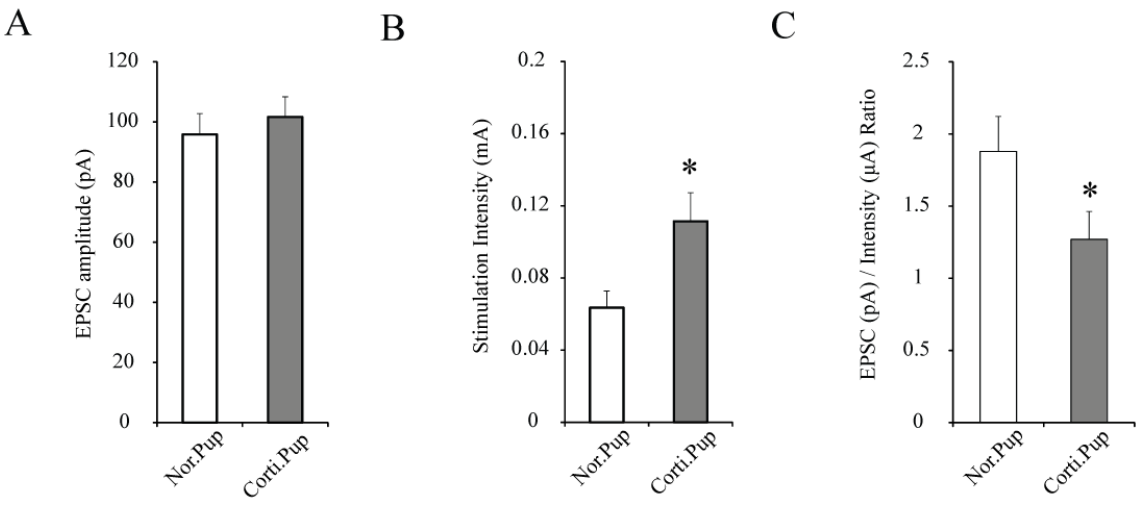

Figure 22. Corti.Pups required stronger stimulation to induce EPSCs as large as those of Nor.Pups (averaged data).

A. The average of EPSC amplitudes. The amplitudes of EPSCs were experimentally adjusted with 50 to 150 pA. **B.** The average of stimulation intensity to evoke similar EPSCs. Corti.Pups required significantly greater stimulations to induce EPSCs. **C.** The averaged ratio of EPSC amplitudes to the stimulation intensity. The ratio of EPSC/intensity in Corti.Pups was significantly lower than that of Nor.Pups. Data indicate the mean ± S.E. *, $p < 0.05$.

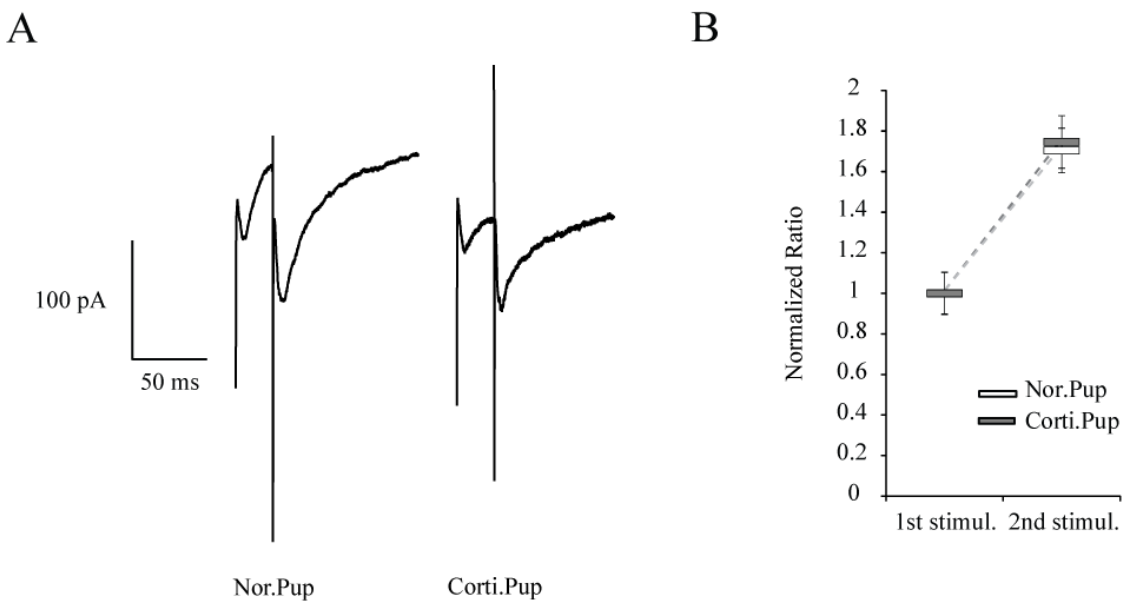

Figure 23. PPFs did not differ between the two groups.

A. Example traces of two EPSCs evoked by two consecutive stimuli with an interval of 50 ms in hippocampal CA1 neurons. **B.** Normalized PPFs. These were not different between two groups, indicating no alterations in presynaptic properties of Corti.Pups.

9. The levels of BDNF in the PFC and HPC during neurodevelopment were lower in Corti.Pups and Nor.Pups

I have previously reported that elevating maternal cortisol levels during pregnancy significantly influenced cortisol levels of offspring measured postnatally [11]. As described above, I observed incomplete LTP formation and aberrant switching of the NR2B to NR2A subunits in Corti.Pups. Moreover, the postsynaptic response was weaker in Corti.Pups than in Nor.Pups, suggesting a delay and/or dysregulation in the neurodevelopmental processes in Corti.Pups. Therefore, I tried to compare the expression levels of BDNF, a well-established regulator of neurodevelopment. ELISA assay of relative BDNF expression levels in PFC and HPC tissues extracted from postnatal day 7, 14 and 21 brains, revealed that BDNF levels in both brain areas were significantly lower in Corti.Pups than in Nor.Pups (Fig. 24, BDNF level in Prefrontal cortex, p7, Nor.Pup = 50.12 ± 1.42 , n = 6; Corti.Pup = 20.36 ± 1.82 , n = 8; $p < 0.01$; p14, Nor.Pup = 97.14 ± 2.52 , n = 9; Corti.Pup = 94.21 ± 8.58 , n = 6; n.s; p21, Nor.Pup = 71.19 ± 3.27 , n = 6; Corti.Pup = 41.77 ± 1.90 , n = 8; $p < 0.01$; BDNF level in Hippocampus, p7, Nor.Pup = 89.17 ± 2.12 , n = 6; Corti.Pup = 49.68 ± 3.17 , n = 8; $p < 0.01$; p14, Nor.Pup = 222.95 ± 5.76 , n = 9; Corti.Pup = 176.95 ± 6.28 , n = 6; $p < 0.01$; p21, Nor.Pup = 92.24 ± 2.89 , n = 6; Corti.Pup = 58.20 ± 1.49 , n = 8; $p < 0.01$). These results suggested that abnormally elevated cortisol levels during the neonatal period negatively affected the expression of BNDF, which is necessary for brain development.

A

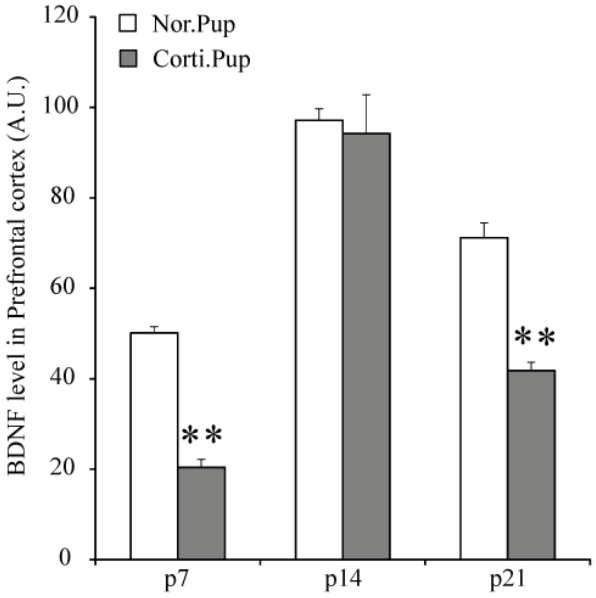

B

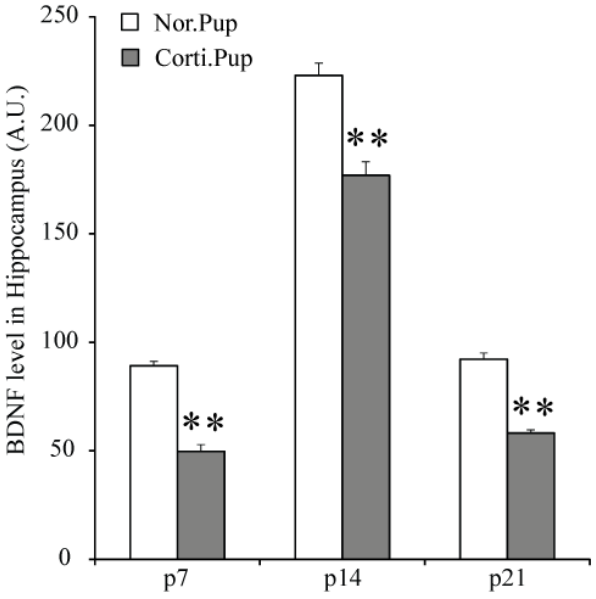

Figure 24. BDNF levels were significantly lower in Corti.Pups than in Nor.Pups.

A. The average of BDNF levels measured in PFC. These were significantly lower in postnatal 7 and 21 in PFC of Corti.Pups. **B.** The average of BDNF levels measured in HPC. These were significantly lowered in Corti.Pups during postnatal three weeks. Data indicate the mean ± S.E. **, $p < 0.01$, compared with each other group.

10. The expression of major factors for synaptic developments was downregulated by high cortisol

It was confirmed that BDNF expression in brain tissues was lower in Corti.Pups than in Nor.Pups. Next, to compare the expression levels of BDNF-regulated/regulating proteins implicated in neurodevelopment between Corti.Pups and Nor.Pups, PFC and HPC tissues were extracted from postnatal day 1 brains, and the amount of proteins in each tissue was analyzed using Western blot. I first measured the expression levels of mTOR, which is involved in growth and metabolic regulation of eukaryotic cells, and then its upstream regulator, PKA. I confirmed that in PFC, the expression levels of both mTOR and PKA were significantly lower in Corti.Pups than in Nor.Pups, while no difference was observed in HPC tissues (Fig. 25 and 26, % of mTOR, Hippocampus, Nor.Pup = 100 ± 15.97 %, n = 8; Corti.Pup = 115.98 ± 20.64 %, n = 8; n.s; Prefrontal cortex, Nor.Pup = 100 ± 11.54 %, n = 8; Corti.Pup = 51.40 ± 8.80 %, n = 8; $p < 0.01$; % of PKA, Hippocampus, Nor.Pup = 100 ± 10.79 %, n = 8; Corti.Pup = 106.29 ± 11.49 %, n = 8; n.s; Prefrontal cortex, Nor.Pup = 100 ± 8.15 %, n = 8; Corti.Pup = 54.78 ± 7.37 %, n = 8; $p < 0.01$). These results provided evidence that the structural and functional development of brain was impaired due to prenatal exposure to high cortisol levels.

A

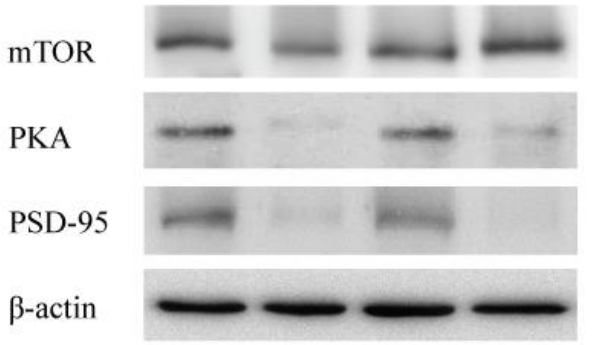

B

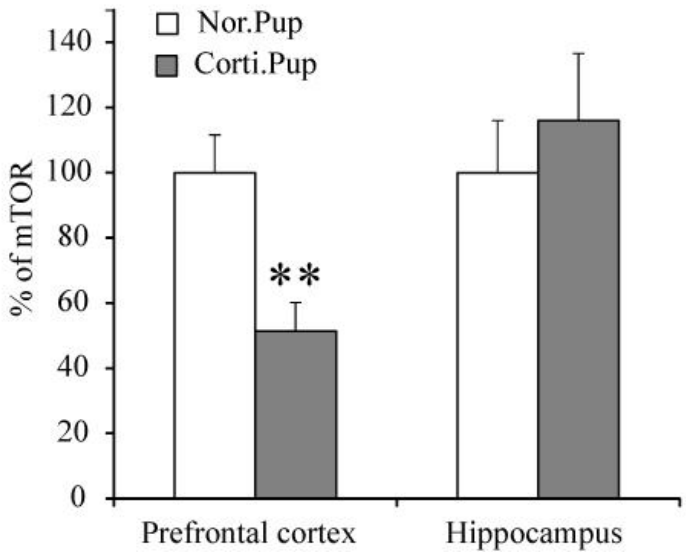

Figure 25. mTOR was significantly lower in the PFC of Corti.Pups.

A. Data show protein expression patterns of mTOR, PKA and PSD-95 in PFC and HPC between the two groups. **B.** mTOR was significantly lower in the PFC of Corti.Pups, indicating that cortisol-mediated dysregulation may affect brain development. Data indicate the mean ± S.E. **, $p < 0.01$.

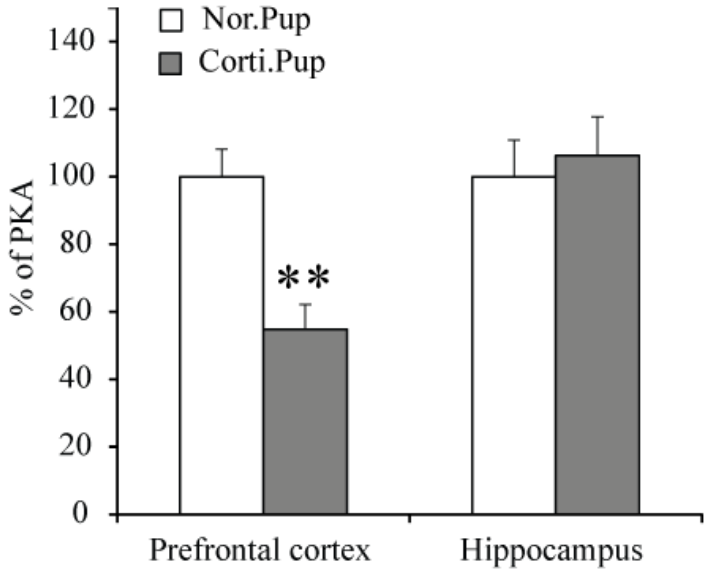

Figure 26. PKA was significantly lower in the PFC of Corti.Pups.

PKA expression was significantly lower in the PFC of Corti.Pups, indicating that cortisol-mediated dysregulation negatively affects developmental Ca^{2+} signaling. Data indicate the mean ± S.E. **, $p < 0.01$.

11. PSD-95 expression was lower in the PFC and HPC of Corti.Pups

The notable decrease in expression levels of BDNF, PKA, and mTOR, which play dominant roles in the neurodevelopmental process, suggested a possibility of abnormal synaptic development in Corti.Pups. Additionally, the electrophysiological results of LTP patterns, NMDAR switching and AMPAR-mediated EPSCs indicated abnormal development of postsynaptic sites in Corti.Pups. Therefore, the expression levels of PSD-95 were measured using Western blot and compared with each other group. As a result, PSD-95 expression levels in PFC and HPC were significantly lower in Corti.Pups than in Nor.Pups (Fig. 27, % of PSD-95, Prefrontal cortex, Nor.Pup = 100 ± 14.14 %, n = 8; Corti.Pup = 63.43 ± 12.66 %, n = 8; $p < 0.05$; Hippocampus, Nor.Pup = 100 ± 15.78 %, n = 8; Corti.Pup = 48.85 ± 22.26 %, n = 8; $p < 0.05$). These results suggested that downregulation of G protein-coupled receptor (GPCR) signaling might occur due to lower PKA expression in Corti.Pups. And then, the downregulation of mTOR and expression of cAMP response element-binding protein (CREB) may have contributed to a decrease in BDNF and PSD-95 expression. This serial cascade of neurodevelopmental downregulation in Corti.Pups may explain why Corti.Pups exhibited incomplete memory formation and synaptic switching (Fig. 11 and 13).

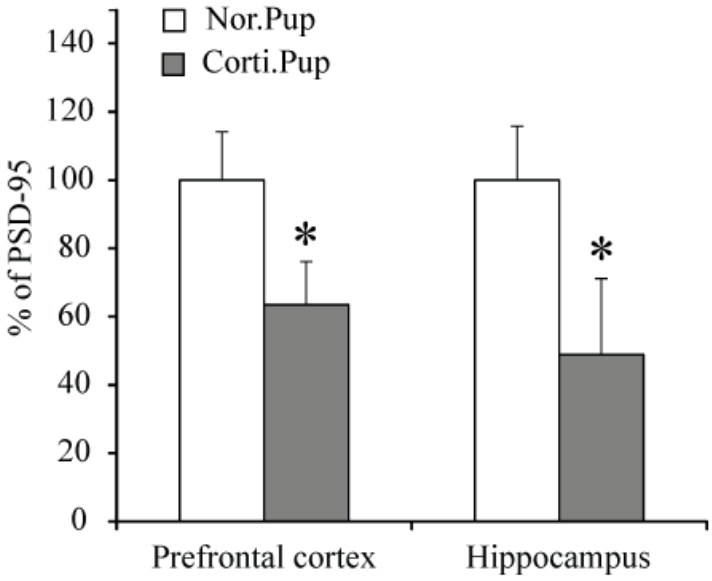

Figure 27. PSD-95 in the PFC and HPC was significantly lower in Corti.Pups.

PSD-95 was significantly less expressed in PFC and HPC of Corti.Pups, indicating that cortisol-mediated dysregulation negatively affects synaptic development and function. Data indicate the mean ± S.E. *, $p < 0.05$.

12. cAMP levels in PFC of were significantly lower in Corti.Pups than in Nor.Pups

Since PKA downregulation seemed to result in a decrease of PSD-95, I needed to investigate the downregulation of cAMP which activates GPCRs responsible for intracellular signaling. Using ELISA assay, the expression levels of cAMP in the PFC and HPC of postnatal day 1 pups were compared between Nor.Pups and Corti.Pups. cAMP expression levels in the PFC were significantly lower in Corti.Pups than in Nor.Pups, while there was no difference in the HPC (Fig. 28, cAMP level in Hippocampus, Nor.Pup = 1.87 ± 0.0055, n = 12; Corti.Pup = 1.86 ± 0.0078, n = 12; n.s; cAMP level in Prefrontal cortex, Nor.Pup = 1.81 ± 0.0073, n = 12; Corti.Pup = 1.74 ± 0.014, n = 12; $p < 0.01$). These results suggested that PKA downregulation due to a decrease of cAMP expression might negatively affect downstream cellular signaling, resulting in postsynaptic dysfunction in Corti.Pups.

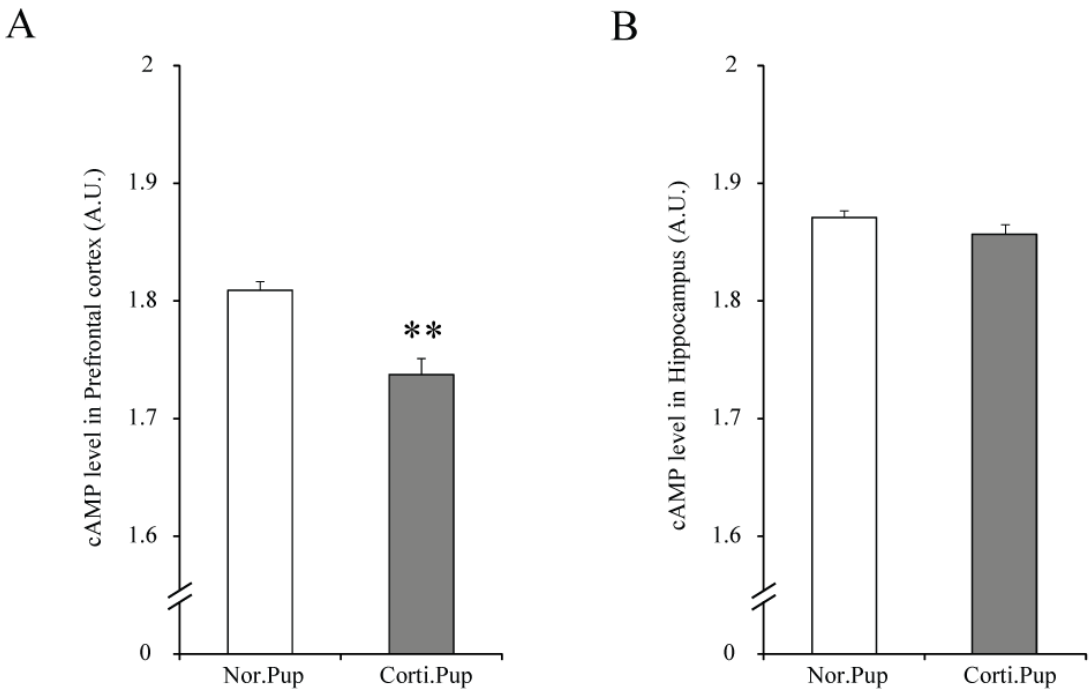

Figure 28. cAMP, an upstream regulator of PKA, was significantly lower in PFC of Corti.Pups.

A. The average of cAMP levels measured in PFC. Corti.Pups showed significantly less cAMP expression in PFC. **B.** The average of cAMP levels measured in HPC. There was no difference between two groups. This indicates that cAMP/PKA interaction may be especially downregulated in PFC of Corti.Pups. Data indicate the mean ± S.E. **, $p < 0.01$.

4. DISCUSSION

I have previously reported that Corti.Pups born from rat mothers treated with continuous corticosterone (20 mg/kg) injection during pregnancy, exhibited increased plasma cortisol levels, deficits of spatial cognitive functions, and ADHD-like behaviors during the post-weaning period [11]. In this study, I aimed to investigate the cellular mechanism of cognitive dysfunction caused by neurodevelopmental impairment, which was induced by prenatal exposure to high cortisol levels. To this end, I performed behavioral experiments to test learning and memory functions in juvenile rat pups, electrophysiological studies to evaluate synaptic function and cell-physiological studies to measure the expression of neurodevelopment-associated proteins. My results demonstrated that Corti.Pups exposed to high cortisol levels, exhibited behavioral deficits in learning and memory formation, incomplete synaptic LTP in CA1 neurons, and delayed postsynaptic development at the neuronal level. The characteristics of Corti.Pups different from Nor.Pups are summarized as follows. 1) Corti.Pups exhibited deficits in long-term memory formation after learning tasks as indicated by longer time and distance to escape in the third MWM test. 2) Target quadrant and annulus times were not reduced in the third MWM test unlike Nor.Pups, indicating reduced attention and learning ability. 3) In the OF test, Corti.Pups exhibited hyperactive behaviors with less adaptability, as indicated by longer moving distances in the total and center areas and faster velocity compared to those in Nor.Pups. 4) In electrophysiological studies using whole-cell patch clamping with postnatal days 13 ~ 18 hippocampal slices, synaptic LTP formation of CA1 neurons was impaired in Corti.Pups. 5) In electrophysiological analysis of the synaptic composition of NMDAR subunits, an ifenprodil-

sensitive component was more observed in Corti.Pups than in Nor.Pups. 6) The amplitude of AMPAR-mediated EPSCs was smaller in Corti.Pups than in Nor.Pups under the same intensity of stimulation. 7) In cell physiology experiments, the expression levels of BDNF, mTOR, PKA, PSD-95, and cAMP, which are critical for neuronal development, in the PFC were significantly lower in Corti.Pups than in Nor.Pups. 8) Expressions of BDNF and PSD-95, which are important for the expression of postsynaptic receptors, in the HPC were lower in Corti.Pups than in Nor.Pups.

The MWM test is a representative experimental technique for evaluating memory formation through cognitive learning and repetitive tasks. In this test, rodents are required to find a hidden platform in a swimming pool and results are closely associated with NMDAR-dependent synaptic plasticity of the HPC at the cellular level [27]. According to the results acquired from the MWM test in this study, Corti.Pups exhibited significantly longer escape time and moving distance to find the hidden platform in the third test performed 24 hours after the first test, compared with Nor.Pups. This strongly implied incomplete formation of long-term memory. This memory impairment was consistent with the results reported by previous studies demonstrating behavioral patterns of Alzheimer's disease model mice with cognitive dysfunction [31, 32]. Specifically, both groups in this study did not exhibit any differences in their performance to find the hidden platform in the second test executed 10 minutes after the first test, indicating that Corti.Pups did not have deficits in short-term memory formation. However, Corti.Pups failed to exhibit complete long-term memory formation in the third test after 24 hours (Fig. 2 and 3). Nevertheless, in both the current and previous studies, the temporal difference between short- and long-term components of learning and memory was not clearly defined. However, only Nor.Pups but not Corti.Pups maintained the memory formation in the third test after 24 hours, indicating that memory consolidation was induced normally in

Nor.Pups after short-term memory formation. This result observed in Nor.Pups was consistent with previous studies reporting that memory consolidation after learning is required for the long-lasting memory formation [33-35]. These findings clearly suggest a possibility that memory consolidation after short-term memory formation did not occur in Corti.Pups. There is a previous report separately evaluating distinct behavioral performance according to short- and long-term memory formation in adult rats with postoperative cognitive dysfunction caused by sevoflurane anesthesia [36]. Compared to Nor.Pups, Corti.Pups exhibited anxiolytic behavior and hyperactivity in the MWM test, indicated by significantly longer time and distance in the target quadrant in the third test. Moreover, the longer first annulus time in the third test indicated inferior cognitive ability and attention in Corti.Pups than in Nor.Pups (Fig. 5).

The OF test is a method to evaluate locomotion and anxiety-like behaviors based on the behavioral patterns of rodent models by exposing them to a novel open space. This enables observation of behavioral changes that are associated with stress-induced anxiety disorders [37, 38]. The moving distances of two groups demonstrated a decreasing tendency over repetitive trials, but Corti.Pups consistently exhibited a longer moving distance and a faster velocity compared to Nor.Pups. These results revealed hyperactivity patterns that were consistent with the MWM test results. Furthermore, analysis of the center ratio indicated that Corti.Pups lacked adaptive ability to a novel environment (Fig. 8 and 9). As shown in Figure 9A, the center distance/total distance ratios of Corti.Pups remained consistently high without a significant reduction of center moving distance over three days, indicating their anxiety-like behaviors. In contrast, Nor.Pups demonstrated a significant reduction in center/total ratio on the second test day, indicating proper adaptation to the OF environment. On the third test day, the center/total ratio again increased in Nor.Pups because the total distance decreased significantly in the final experiment together with a reduction of center moving distance. In this regard, the different

behavioral patterns of juvenile Corti.Pups observed in the MWM and OF tests suggest possibly abnormalities in neurophysiological functions in both the PFC and HPC.

A number of neuroscientists have attempted to electrophysiologically identify the cellular mechanisms of memory formation in associated with behavioral patterns in the MWM test. For example, in a previous study evaluating the memory function of adolescent rats following early maternal separation-induced stresses, EPSP-LTP in the HPC was incomplete and spatial learning and memory function in the MWM test were impaired [39]. The other study examining the effects of intracerebroventricular injection of gangliosides, which are major components of the cell membrane related to neurophysiological function, revealed improvements in spatial learning and memory in the MWM test and ATP-induced LTP of hippocampal CA1 neurons in rats [40]. Furthermore, the modulation of synaptic plasticity is closely associated with neuropsychiatric and neurodegenerative diseases. Previous reports have demonstrated that stress attenuated LTP in the rodent hippocampi, and synaptic toxicity of amyloid-β peptide caused excessive increase in intracellular Ca^{2+} via activation of endoplasmic reticulum and NMDARs, thereby attenuating LTP and PSD-95 function in Alzheimer's disease [41-43]. Additionally, it was reported that LTP induction in hippocampal CA1 neurons weakened by exposure to corticosterone was restored by inhibiting the increase of intracellular Zn^{2+} with effusol treatment [44]. Therefore, it was necessary to elucidate the cellular mechanisms underlying the deterioration in learning and memory of Corti.Pups observed in the MWM test by measuring LTP patterns of hippocampal CA1 neurons. In this experiment, I demonstrated that the synaptic plasticity of CA1 neurons were crucially weakened in Corti.Pups during early development, compared to those in Nor.Pups (Fig. 11 and 12).

As a central concept of learning and memory, formation of synaptic LTP is dependent on Ca^{2+} and NMDARs. According to previous studies assessing synaptic plasticities in hippocampi of 2

~ 3-week-old rats, LTP induction initially involved the interaction of calmodulin and Ca^{2+} introduction through NMDARs, and metabotropic glutamate receptor-dependent long-term depression was induced by intracellular Ca^{2+} influx through L-type Ca^{2+} channels without NMDAR activation [45, 46]. NMDARs consist of two obligatory NR1 subunits and two regulatory subunits. As a regulatory component, NR2B subunits are highly expressed in NMDARs immediately after birth. Throughout development, these subunits are gradually replaced with NR2A subunits within postnatal 3 weeks [47]. In a previous study, NMDARs containing NR2A or NR2B subunits played a critical role to determine the direction of synaptic plasticity [48]. One study examined the contribution of NR2A- or NR2B-containing NMDARs to LTP induction in corticostriatal slices of 13 ~ 14-day-old rats and reported that induction of LTP by a high-frequency protocol required the activation of NR2A-containing NMDARs, but not NR2B-containing NMDARs [49]. In addition, a study on the regulation of Rabphilin3A (Rph3A), which participates in stabilization of NMDARs in postsynaptic membranes via forming a complex of NR2A and PSD-95, reported that inhibition of Rph3A and NR2A/Rph3A complex blocked LTP induction as well as spatial memory [50]. Thus, although still remains controversial, NR2A subunits after developmental switching are required for the induction of synaptic LTP in hippocampal CA1 neurons at postnatal weeks 2 ~ 3. In this study, the higher ifenprodil-sensitivity of NMDAR-EPSCs in CA1 neurons of Corti.Pups indirectly implies higher expression of NR2B-containing receptors in postsynaptic sites, suggesting impaired subunit switching (Fig. 14). Since NMDAR subunit switching is a key process in postsynaptic development and for synaptic plasticity, it is likely that the incomplete LTP observed in Corti.Pups was attributed to the impaired switching of NMDAR subunits.

In these electrophysiological experiments comparing the neuronal membrane properties between the two groups, I did not focus on the kinetics of specific membrane proteins to

dominantly determine membrane properties and excitability, although I observed differences in WC, AP threshold, firing rates in depolarization and voltage sags in hyperpolarization. Membrane proteins such as ion channels and receptors play functionally critical roles to regulate membrane excitability in neurons. The activation of many types of ion channels and receptors are involved in the regulation of neuronal osmotic pressure and loss of ion homeostasis. Particularly, Na^+ channels and glutamate-gated ionotropic NMDARs or AMPARs are key pathways for ions flux during neuronal damages [51]. Therefore, it is possible that membrane functions to regulate intracellular components were downregulated in Corti.Pups, which exhibited a higher WC with no difference in R_{in} (Fig. 15 ~ 17 and 20). Additionally, the lower AP threshold in Corti.Pups possibly indicates the existence of differences in composition and substrate characteristics of Na^+ channels and A-type K^+ channels [29]. More details about these issues should be addressed in further studies. The significantly lower firing rates of APs in CA1 neurons of Corti.Pups suggest that the distribution of cation channels may differ between groups (Fig. 17). The significant difference between the two groups was also observed at the subthreshold level. Smaller voltage sags during membrane hyperpolarization were observed in Corti.Pups, compared with those in Nor.Pups, suggesting lower expression of I_h channels in Corti.Pups (Fig. 20) [30]. One previous report demonstrated that the membrane properties of neurons were predominantly determined by lipid-protein interactions in the plasma membrane. Phosphatidylserine in the cell membrane stabilized Na^+-K^+ ATPase, but phosphatidylcholine or phosphatidylethanolamine rendered them unstable [52]. In this regard, the similarity in membrane R_{in} of CA1 neurons between the two groups, even with differences in firing rates and voltage sags, suggests further analysis to identify not only membrane proteins but also lipid substrates.

As previously mentioned, synaptic transmission and plasticity are dependent on both pre- and

postsynaptic Ca^{2+} modulation in CA1 neurons [53]. In this study, I confirmed that compared to Nor.Pups, the greater intensity of stimulation was required to produce the similar amplitude of EPSCs in Corti.Pups (Fig. 22). However, the PPFs of EPSCs did not exhibit any differences between the two groups, suggesting that the presynaptic release of neurotransmitters were similar between groups [54]. In conjunction with the results of NMDAR composition shown in Figure 14, these results indicate possible impairment of postsynaptic functions in Corti.Pups.

Steroid-mediated dysregulation of the neuroendocrine system, which affects neurodevelopment, is involved in ADHD pathogenesis. Accordingly, it is crucial to target the changes of major factors regulating intracellular signaling cascades of neurodevelopment in PFC and HPC. BDNF, a major factor that regulates neurodevelopment, plays crucial roles in neuronal formation and growth, synaptic plasticity, and neuroprotective mechanisms during brain development. BDNF activates cAMP via the PKA-CREB-BDNF signaling cascade, which then activates the mTOR complex1 that regulates protein synthesis and cellular metabolism in neurons [55-57]. In particular, a previous study investigating the relationship between endocrine dysregulation and biological markers in patients with type-2 diabetes and depression, reported a close correlation between increased blood cortisol levels and decreased BDNF levels [58]. Furthermore, abnormal regulation of the neuroendocrine system was observed in neuropsychiatric diseases caused by environmental factors. A previous study examining the pathogenesis of ADHD and ASD caused by fine particulate matter pollution, reported a decrease in neuronal viability and downregulation of PKA and CREB phosphorylation by the toxic effects of pollution in the HPC of animal models. Further, neuronal apoptosis and synaptic damages were dramatically alleviated by increasing the expression of PKA, CREB and BDNF [59]. Another report investigated the antidepressant effects of *Adansonia digitata L.*, to reverse the dysregulation of the neuroendocrine system. In a CUMS mouse model of depression, *Adansonia*

digitata L., exhibited antidepressant effects by increasing BDNF levels and decreasing blood cortisol levels in a dose-dependent manner, thereby reducing depressive behavioral patterns in the OF, sucrose preference, tail suspension, and novel object recognition tests [19]. In this study, I provided evidence that abnormal signaling cascades in neurons might be due to the neuroendocrine dysregulation during neuronal development, thus negatively affecting postsynaptic development and LTP formation in Corti.Pups. BDNF was significantly decreased in both the PFC and HPC of Corti.Pups, suggesting the existence of physiological and structural deficits in synapses (Fig. 24). In particular, there is a possibility that BNDF-mediated abnormalities in the PFC might cause ADHD-like behaviors and cognitive decline in Corti.Pups. Consistent with these results, it has been reported that maternal stress during pregnancy increased the risk of fetal neurodevelopmental and postnatal neuropsychiatric problems correlated with the PFC and HPA-axis [60]. Moreover, it is well-established that monoaminergic dysfunction in the PFC is associated with ADHD, BD, PTSD, and depression. In particular, it has been previously reported that dopaminergic dysregulation in the PFC of female rats during early adolescent was strongly involved in ADHD pathogenesis [61]. In contrast, in a clinical study examining the role of the HPA axis in patients with ADHD, cortisol levels were lower in patients with ADHD than in healthy controls. Consequently, this phenomenon was due to downregulation of the HPA axis [62]. Taken together, these findings indicate that exposure to high cortisol levels during brain development can induce dysregulation of the neuroendocrine system, affecting the functional and structural formation of synapses during development of the rodent brain. The development of synaptic structure is completed before birth. During this period, a major protein that plays a critical role in the complete formation of synaptic structure is PSD-95, whose expression is regulated by BDNF. In this study, I confirmed lower expression of PSD-95 in the PFC and HPC of Corti.Pups (Fig.27). Accordingly, I quantified expression levels of mTOR and PKA, which act upstream of BDNF and PSD-95. In the comparison of protein

expression levels between Nor.Pups and Corti.Pups, I confirmed that PKA and mTOR expression in the PFC was significantly lower in Corti.Pups than in Nor.Pups. However, their expressions in HPC did not differ between the two groups (Fig. 25 ~ 27). In the HPC of Corti.Pups, the lower expression levels of BDNF and PSD-95, but not PKA and mTOR suggest the existence of another signaling pathway that regulates hippocampal development (Fig. 27). Consequently, this may explain the decreased postsynaptic function of hippocampal CA1 neurons in Corti.Pups. According to immunofluorescence analysis in a previous report, the expression of NR2A and PSD-95 in CA1, CA3, and DG neurons of rat hippocampi were gradually but critically increased at postnatal day 0 to 56, highlighting the importance of PSD-95 in hippocampal development [63]. The postsynaptic downregulation of CA1 neurons induced by the lower expression of PSD-95 in Corti.Pups is consistent with previous results observed in CA1 neurons of damaged hippocampi that occurred memory dysfunction [64]. Moreover, in a previous report on learning and memory impairments caused by perinatal hypoxia, the reduction of PSD-95 and NMDAR subunits by CREB phosphorylation in CA1 neurons on postnatal day 10 was crucially associated with the deterioration in long-term spatial learning and memory, which was restored by D1/D5R activation [65]. Taken together, the lower expression of BDNF and PSD-95 and higher expression of NR2B-containing NMDARs in HPC of Corti.Pups may be the major factors disrupting synaptic LTP. Accordingly, these results suggest a possibility that cortisol-mediated dysregulation of neuroendocrine system negatively affects the expression of neurodevelopment-associated proteins, resulting in developmental deficits in the brain regions involved in cognitive learning and memory function. Indeed, there is experimental and clinical evidence that cortisol-induced dysregulation of the HPA-axis and abnormal D1R expression in the PFC, which downregulates downstream pathways, may lead to neurodevelopmental psychiatric disorders such as ADHD [65, 66].

In this study, I confirmed that the expression levels of cAMP and PKA, which are key players during PFC development, were downregulated by excessive cortisol, and the expression levels of mTOR, PSD-95 and BDNF were also decreased in Corti.Pups (Fig. 26 and 28). These cortisol-induced negative effects possibly cause incomplete synaptic plasticity by perturbing synaptic development in major brain loci in Corti.Pups, thus triggering the pathogenesis of neurodevelopmental psychiatric disorders such as ADHD (Figure 29). Further studies on monoaminergic regulation and associated signaling that are involved in the pathogenesis of neurodevelopmental neuropsychiatric disorders, may reveal novel therapeutic mechanisms through focusing on major factors that contribute to neurodevelopmental signaling cascades and neuroendocrine regulation.

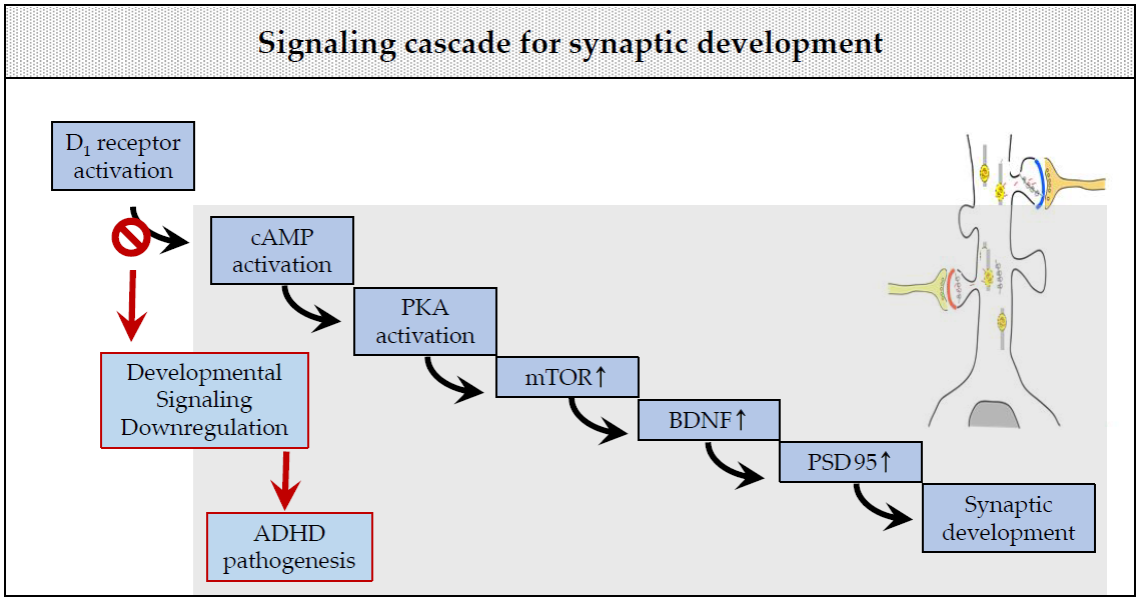

Figure 29. An expected pathogenic mechanism of neurodevelopmental disorder induced by cortisol dysregulation during brain development.

5. REFERENCE

1. Piwowarska J, Chimiak A, Matsumoto H, Dziklińska A, Radziwoń-Zaleska M, Szelenberger W, Pachecka J, Serum cortisol concentration in patients with major depression after treatment with fluoxetine. *Psychiatry Res*, 2012. **198**(3): p. 407-11.
2. Jia Y, Liu L, Sheng C, Cheng Z, Cui L, Li M, Zhao Y, et al., Increased Serum Levels of Cortisol and Inflammatory Cytokines in People With Depression. *J Nerv Ment Dis*, 2019. **207**(4): p. 271-276.
3. Mayer SE, Lopez-Duran NL, Sen S, Abelson JL, Chronic stress, hair cortisol and depression: A prospective and longitudinal study of medical internship. *Psychoneuroendocrinology*, 2018. **92**: p. 57-65.
4. Qin DD, Rizak J, Feng XL, Yang SC, Lü LB, Pan L, Yin Y, et al., Prolonged secretion of cortisol as a possible mechanism underlying stress and depressive behaviour. *Sci Rep*, 2016. **6**: p. 30187.
5. Gomez RG, Posener JA, Keller J, DeBattista C, Solvason B, Schatzberg AF, Effects of major depression diagnosis and cortisol levels on indices of neurocognitive function. *Psychoneuroendocrinology*, 2009. **34**(7): p. 1012-8.
6. Bozkurt H, Şimşek Ş, Şahin S, Elevated levels of cortisol, brain-derived neurotropic factor and tissue plasminogen activator in male children with autism spectrum disorder. *Autism Res*, 2021. **14**(10): p. 2078-2084.

7. Courtemanche AB, Black WR, Meyer JS, Hair Cortisol and Self-Injurious Behavior Among Children With Autism Spectrum Disorder. *Am J Intellect Dev Disabil*, 2021. **126**(2): p. 158-166.

8. Koumantarou Malisiova E, Mourikis I, Darviri C, Nicolaides NC, Zervas IM, Papageorgiou C, Chrousos GP, Hair cortisol concentrations in mental disorders: A systematic review. *Physiol Behav*, 2021. **229**: p. 113244.

9. Zorn JV, Schür RR, Boks MP, Kahn RS, Joëls M, Vinkers CH, Cortisol stress reactivity across psychiatric disorders: A systematic review and meta-analysis. *Psychoneuroendocrinology*, 2017. **77**: p. 25-36.

10. Wichmann S, Kirschbaum C, Böhme C, Petrowski K, Cortisol stress response in post-traumatic stress disorder, panic disorder, and major depressive disorder patients. *Psychoneuroendocrinology*, 2017. **83**: p. 135-141.

11. Jeon SC, Kim HJ, Ko EA, Jung SC, Prenatal Exposure to High Cortisol Induces ADHD-like Behaviors with Delay in Spatial Cognitive Functions during the Post-weaning Period in Rats. *Exp Neurobiol*, 2021. **30**(1): p. 87-100.

12. Kozłowska A, Wojtacha P, Równiak M, Kolenkiewicz M, Tsai ML, Differences in serum steroid hormones concentrations in Spontaneously Hypertensive Rats (SHR) - an animal model of Attention-Deficit/Hyperactivity Disorder (ADHD). *Physiol Res*, 2019. **68**(1): p. 25-36.

13. Ellenbogen MA, Hodgins S, Linnen AM, Ostiguy CS, Elevated daytime cortisol levels: a biomarker of subsequent major affective disorder? *J Affect Disord*, 2011. **132**(1-2): p. 265-9.

14. Nandam LS, Brazel M, Zhou M, Jhaveri DJ, Cortisol and Major Depressive Disorder-Translating Findings From Humans to Animal Models and Back. *Front Psychiatry*, 2019. **10**: p. 974.

15. Kennis M, Gerritsen L, van Dalen M, Williams A, Cuijpers P, Bockting C, Prospective biomarkers of major depressive disorder: a systematic review and meta-analysis. *Mol Psychiatry*, 2020. **25**(2): p. 321-338.

16. Barfield ET and Gourley SL, Prefrontal cortical trkB, glucocorticoids, and their interactions in stress and developmental contexts. *Neurosci Biobehav Rev*, 2018. **95**: p. 535-558.

17. Yu ZY, Wrange O, Boethius J, Gustafsson JA, Granholm L, A qualitative comparison of the glucocorticoid receptor in cytosol from human brain and rat brain. *Brain Res*, 1981. **223**(2): p. 325-33.

18. Dong D, Lei T, Song M, Ma L, Zhao H, The antidepressant effects of l-arginine on chronic mild stress-induced depression by augmenting the expression of brain-derived neurotrophic factor in rats. *Brain Res Bull*, 2020. **158**: p. 128-134.

19. Shehu A, Magaji MG, Yau J, Ahmed A, Methanol stem bark extract of Adansonia digitata ameliorates chronic unpredictable mild stress-induced depression-like behavior: Involvement of the HPA axis, BDNF, and stress biomarkers pathways. *J Basic Clin Physiol Pharmacol*, 2019. **30**(3).

20. Zhang B, Guo F, Ma Y, Song Y, Lin R, Shen FY, Jin GZ, et al., Activation of D1R/PKA/mTOR signaling cascade in medial prefrontal cortex underlying the antidepressant effects of l-SPD. *Sci Rep*, 2017. **7**(1): p. 3809.

21. Marsden WN, Synaptic plasticity in depression: molecular, cellular and functional correlates. *Prog Neuropsychopharmacol Biol Psychiatry*, 2013. **43**: p. 168-84.

22. Jiang R, Babyak MA, Brummett BH, Siegler IC, Kuhn CM, Williams RB, Brain-derived neurotrophic factor (BDNF) Val66Met polymorphism interacts with gender to influence cortisol responses to mental stress. *Psychoneuroendocrinology*, 2017. **79**: p. 13-19.

23. Brummett BH, Babyak MA, Kuhn CM, Siegler IC, Williams RB, A functional polymorphism in the HTR2C gene associated with stress responses: a validation study. *Biol Psychol*, 2014. **103**: p. 317-21.

24. Brummett BH, Kuhn CM, Boyle SH, Babyak MA, Siegler IC, Williams RB, Cortisol responses to emotional stress in men: association with a functional polymorphism in the 5HTR2C gene. *Biol Psychol*, 2012. **89**(1): p. 94-8.

25. Williams RB, Marchuk DA, Gadde KM, Barefoot JC, Grichnik K, Helms MJ, Kuhn CM, et al., Central nervous system serotonin function and cardiovascular responses to stress. *Psychosom Med*, 2001. **63**(2): p. 300-5.

26. Williams RB, Marchuk DA, Siegler IC, Barefoot JC, Helms MJ, Brummett BH, Surwit RS, et al., Childhood socioeconomic status and serotonin transporter gene polymorphism enhance cardiovascular reactivity to mental stress. *Psychosom Med*, 2008. **70**(1): p. 32-9.

27. Vorhees CV and Williams MT, Morris water maze: procedures for assessing spatial and related forms of learning and memory. *Nat Protoc*, 2006. **1**(2): p. 848-58.

28. Bliss TV and Collingridge GL, A synaptic model of memory: long-term potentiation in the hippocampus. *Nature*, 1993. **361**(6407): p. 31-9.

29. Jung SC and Hoffman DA, Biphasic somatic A-type K channel downregulation mediates intrinsic plasticity in hippocampal CA1 pyramidal neurons. *PLoS One*, 2009. **4**(8): p. e6549.

30. Yang YS, Kang MS, Kim SH, Kim SJ, Eun SY, Kwon OB, Jung SC, I(h) channels prevent overexcitability of early developmental CA1 neurons showing high input resistance in rats. *Brain Res Bull*, 2013. **91**: p. 14-20.

31. Bromley-Brits K, Deng Y, Song W, Morris water maze test for learning and memory deficits in Alzheimer's disease model mice. *J Vis Exp*, 2011(53).

32. Curdt N, Schmitt FW, Bouter C, Iseni T, Weile HC, Altunok B, Beindorff N, et al., Search strategy analysis of Tg4-42 Alzheimer Mice in the Morris Water Maze reveals early spatial navigation deficits. *Sci Rep*, 2022. **12**(1): p. 5451.

33. Remondes M and Schuman EM, Role for a cortical input to hippocampal area CA1 in the consolidation of a long-term memory. *Nature*, 2004. **431**(7009): p. 699-703.

34. Coles K and Tomporowski PD, Effects of acute exercise on executive processing, short-term and long-term memory. *J Sports Sci*, 2008. **26**(3): p. 333-44.

35. Wally ME, Nomoto M, Abdou K, Murayama E, Inokuchi K, A short-term memory trace persists for days in the mouse hippocampus. *Commun Biol*, 2022. **5**(1): p. 1168.

36. Karaman T, Karaman S, Doğru S, Tapar H, Şahin A, Süren M, Short-Term and Long-Term Effects of Dexamethasone on Cognitive Dysfunction Induced by Sevoflurane in Adult Rats. *Turk J Anaesthesiol Reanim*, 2017. **45**(3): p. 158-163.

37. Kraeuter AK, Guest PC, Sarnyai Z, The Open Field Test for Measuring Locomotor Activity and Anxiety-Like Behavior. *Methods Mol Biol*, 2019. **1916**: p. 99-103.

38. Sturman O, Germain PL, Bohacek J, Exploratory rearing: a context- and stress-sensitive behavior recorded in the open-field test. *Stress*, 2018. **21**(5): p. 443-452.

39. Cao X, Huang S, Cao J, Chen T, Zhu P, Zhu R, Su P, et al., The timing of maternal separation affects morris water maze performance and long-term potentiation in male rats. *Dev Psychobiol*, 2014. **56**(5): p. 1102-9.

40. Jung WR, Kim HG, Kim KL, Ganglioside GQ1b improves spatial learning and memory of rats as measured by the Y-maze and the Morris water maze tests. *Neurosci Lett*, 2008. **439**(2): p. 220-5.

41. Howland JG and Wang YT, Synaptic plasticity in learning and memory: stress effects in the hippocampus. *Prog Brain Res*, 2008. **169**: p. 145-58.

42. Popugaeva E, Pchitskaya E, Bezprozvanny I, Dysregulation of neuronal calcium homeostasis in Alzheimer's disease - A therapeutic opportunity? *Biochem Biophys Res Commun*, 2017. **483**(4): p. 998-1004.

43. Tu S, Okamoto S, Lipton SA, Xu H, Oligomeric Aβ-induced synaptic dysfunction in Alzheimer's disease. *Mol Neurodegener*, 2014. **9**: p. 48.

44. Tamano H, Sato Y, Takiguchi M, Murakami T, Fukuda T, Kawagishi H, Suzuki M, et al., CA1 LTP Attenuated by Corticosterone is Canceled by Effusol via Rescuing Intracellular Zn(2+) Dysregulation. *Cell Mol Neurobiol*, 2019. **39**(7): p. 975-983.

45. Wu J, Rush A, Rowan MJ, Anwyl R, NMDA receptor- and metabotropic glutamate receptor-dependent synaptic plasticity induced by high frequency stimulation in the rat dentate gyrus in vitro. *J Physiol*, 2001. **533**(Pt 3): p. 745-55.

46. Gnegy ME, Ca2+/calmodulin signaling in NMDA-induced synaptic plasticity. *Crit Rev Neurobiol*, 2000. **14**(2): p. 91-129.

47. Gray JA, Shi Y, Usui H, During MJ, Sakimura K, Nicoll RA, Distinct modes of AMPA receptor suppression at developing synapses by GluN2A and GluN2B: single-cell NMDA receptor subunit deletion in vivo. *Neuron*, 2011. **71**(6): p. 1085-101.

48. Yashiro K and Philpot BD, Regulation of NMDA receptor subunit expression and its implications for LTD, LTP, and metaplasticity. *Neuropharmacology*, 2008. **55**(7): p. 1081-94.

49. Li P, Li YH, Han TZ, NR2A-containing NMDA receptors are required for LTP induction in rat dorsolateral striatum in vitro. *Brain Res*, 2009. **1274**: p. 40-6.

50. Franchini L, Stanic J, Ponzoni L, Mellone M, Carrano N, Musardo S, Zianni E, et al., Linking NMDA Receptor Synaptic Retention to Synaptic Plasticity and Cognition. *iScience*, 2019. **19**: p. 927-939.

51. LoPachin RM, Gaughan CL, Lehning EJ, Weber ML, Taylor CP, Effects of ion channel blockade on the distribution of Na, K, Ca and other elements in oxygen-glucose deprived CA1 hippocampal neurons. *Neuroscience*, 2001. **103**(4): p. 971-83.

52. Haviv H, Habeck M, Kanai R, Toyoshima C, Karlish SJD, Neutral phospholipids stimulate Na,K-ATPase activity: a specific lipid-protein interaction. *J Biol Chem*, 2013. **288**(14): p. 10073-10081.

53. Padamsey Z, Foster WJ, Emptage NJ, Intracellular Ca(2+) Release and Synaptic Plasticity: A Tale of Many Stores. *Neuroscientist*, 2019. **25**(3): p. 208-226.

54. Clark KA, Randall AD, Collingridge GL, A comparison of paired-pulsed facilitation of AMPA and NMDA receptor-mediated excitatory postsynaptic currents in the hippocampus. *Exp Brain Res*, 1994. **101**(2): p. 272-8.

55. Kowiański P, Lietzau G, Czuba E, Waśkow M, Steliga A, Moryś J, BDNF: A Key Factor with Multipotent Impact on Brain Signaling and Synaptic Plasticity. *Cell Mol Neurobiol*, 2018. **38**(3): p. 579-593.

56. Zhong Y, Chen J, Li L, Qin Y, Wei Y, Pan S, Jiang Y, et al., PKA-CREB-BDNF signaling pathway mediates propofol-induced long-term learning and memory impairment in hippocampus of rats. *Brain Res*, 2018. **1691**: p. 64-74.

57. Bockaert J and Marin P, mTOR in Brain Physiology and Pathologies. *Physiol Rev*, 2015. **95**(4): p. 1157-87.

58. Prabu P, Poongothai S, Shanthirani CS, Anjana RM, Mohan V, Balasubramanyam M, Altered circulatory levels of miR-128, BDNF, cortisol and shortened telomeres in patients with type 2 diabetes and depression. *Acta Diabetol*, 2020. **57**(7): p. 799-807.

59. Liu J, Liu B, Yuan P, Cheng L, Sun H, Gui J, Pan Y, et al., Role of PKA/CREB/BDNF signaling in PM2.5-induced neurodevelopmental damage to the hippocampal neurons of rats. *Ecotoxicol Environ Saf*, 2021. **214**: p. 112005.

60. Van den Bergh BRH, van den Heuvel MI, Lahti M, Braeken M, de Rooij SR, Entringer S, Hoyer D, et al., Prenatal developmental origins of behavior and mental health: The influence of maternal stress in pregnancy. *Neurosci Biobehav Rev*, 2020. **117**: p. 26-64.

61. Illiano P, Leo D, Gainetdinov RR, Pardo M, Early Adolescence Prefrontal Cortex Alterations in Female Rats Lacking Dopamine Transporter. *Biomedicines*, 2021. **9**(2).

62. Chang JP, Su KP, Mondelli V, Pariante CM, Cortisol and inflammatory biomarker levels in youths with attention deficit hyperactivity disorder (ADHD): evidence from a systematic review with meta-analysis. *Transl Psychiatry*, 2021. **11**(1): p. 430.

63. Ling W, Chang L, Song Y, Lu T, Jiang Y, Li Y, Wu Y, Immunolocalization of NR1, NR2A, and PSD-95 in rat hippocampal subregions during postnatal development. *Acta Histochem*, 2012. **114**(3): p. 285-95.

64. Ocampo AC, Squire LR, Clark RE, Hippocampal area CA1 and remote memory in rats. *Learn Mem*, 2017. **24**(11): p. 563-568.

65. Chen WF, Chang H, Wong CS, Huang LT, Yang CH, Yang SN, Impaired expression of postsynaptic density proteins in the hippocampal CA1 region of rats following perinatal hypoxia. *Exp Neurol*, 2007. **204**(1): p. 400-10.

66. Lautarescu A, Craig MC, Glover V, Prenatal stress: Effects on fetal and child brain development. *Int Rev Neurobiol*, 2020. **150**: p. 17-40.

ABSTRACT IN KOREAN

코티졸은 흔히 ‘스트레스 호르몬’이라 불리는데 스트레스를 받을 때 분비량이 증가하며, 정상적으로 조절될 경우 스트레스에 대한 방어기전으로 심폐 활동을 증진해 더 민첩하고 빠르게 행동할 수 있게 하고 혈당을 상승시켜 더 명확하게 판단할 수 있도록 돕지만 스트레스 상황이 만성화되면 혈당과 혈압 상승으로 인해 면역계가 약해져 노화와 질병이 촉진된다. 따라서 만성 스트레스에 의한 지속적인 코티졸 상승은 신경정신과적 질병의 생체 지표로서 많은 연구들에서 활용 되고 있으며 특히, 주요우울장애 뿐만 아니라 주의력결핍 과잉행동장애, 자폐 스펙트럼 장애, 외상후 스트레스 장애 등 다양한 신경정신과적 질병들과도 관련이 있음이 밝혀졌다. 최근, 실험적으로 임신 중 어미쥐의 코티졸 수치를 증가시켰을 때 새끼쥐에게도 혈중 코티졸의 증가가 나타나고 있음이 발표되었으며, 이렇게 태어난 새끼쥐들은 정상군과는 달리 강제 수영 실험, 열린 공간 실험, 십자형 높은 미로 실험, 모리스 수중 미로 실험에서 과잉행동, 새로운 공간에 대한 부적응 및 항불안성, 학습능력 및 기억력의 감소 등 주의력결핍 과잉행동장애와 비슷한 양상을 나타남이 보고되었다. 따라서 본 연구에서 세포생리학적, 전기생리학적 그리고 인지기능행동학적

실험들을 통해 뇌 성장단계에서 모계를 통해 고농도 코티졸에 노출되었을 경우 신경발달성장애, 인지기능장애, 내분비조절장애의 유무와 주의력결핍 과잉행동장애 발병기전과의 연관성을 구체화하고자 하였다. 이를 위하여, 행동실험과 뇌조직을 이용한 전기생리학 실험 및 단백질 발현 등을 확인할 수 있는 세포생리학적 실험을 진행하였으며, 그 결과 고농도의 코티졸에 노출된 새끼 쥐들에게서 인지기능 저하가 나타났으며 이를 통해 세포단위에서의 학습 및 기억 기전뿐만 아니라 해마 신경세포의 후연접 신경발달이 불완전하다는 것을 확인할 수 있었다. 정상군 (Nor.Pup)과 비교했을 때 실험군 (Corti.Pup)에서 확인된 실험적 증거들은 다음과 같다.

1) 모리스 수중 미로 실험 결과, 첫 실험 후 24 시간 뒤 시행된 세 번째 실험에서 다시 증가된 이동거리와 임무수행시간을 통해 반복된 학습 이후 장기 기억이 형성되지 않고 있음. 2) 모리스 수중 미로 실험의 세 번째 실험에서 감소되지 않은 대상 사분면 시간과 첫번째 플랫폼 도착 시간은 주의 집중력 및 학습능력 감소를 의미. 3) 열린 공간 실험 결과 Nor.Pup 보다 상대적으로 긴 이동 거리와 빠른 속도, 감소되지 않은 중앙영역의 이동 거리는 과잉행동 뿐만 아니라 공간에 대한 적응능력이 정상적이지 않음. 4) 출생 후 13 ~ 18 일에 추출된 해마 조직에서 whole-cell voltage clamping 을 이용한 시냅스 가소성을 측정한 실험에서 CA1 신경세포의 장기강화작용이 제대로 형성되지 않고 있음. 5) 장기강화작용 형성에 중요한 시냅스의 수용체 구성을 비교한

결과 신경발달과정에서 일어나야 하는 NMDAR 소단위체의 시냅스 변화가 제대로 이루어지지 않음. 6) 신경세포 간 시냅스 신호전달 특성을 해마의 CA1 신경세포의 EPSC 로 비교한 결과 자극강도 대비 후연접 AMPAR current 가 작음. 7) 세포생리학적 실험을 통해 전두엽 조직에서 신경세포 발달에 중요한 cAMP, PKA, mTOR, BDNF, PSD-95 모두 감소되어 있음. 8) 해마 조직에서 특이적으로 후엽접 막 단백질 발현에 중요한 BDNF, PSD-95 의 감소.

본 연구에서는 임신기간 중 고농도의 코티졸에 노출된 Corti.Pup 에서 코티졸 조절기능 이상으로 전두엽의 발달기간에 중요한 cAMP, PKA 신호전달 단계가 하향조절 되었으며, 이로 인해 mTOR 발현 및 BDNF 농도가 감소된 것을 확인할 수 있었다. 이러한 하향조절은 전두엽 뿐만 아니라 해마 조직에서도 BDNF 의 감소를 일으켰으며 시냅스 형성에 중요한 PSD95 의 발현을 감소시켰다. 따라서 코티졸에 의해 유도된 부정적 영향들이 학습 및 기억기전 발달에 중요한 시기에 Corti.Pup 의 시냅스 가소성 기능장애를 일으켰음을 알 수 있다. 종합적으로 이러한 결과들로 인해 뇌의 주요 부위에서 시냅스 발달이 저하됨으로써 신경발달장애성 신경정신과질환인 주의력결핍 과잉행동장애의 발병을 유도할 수 있을 가능성이 있다. 이후 추가 실험을 통해, 카테콜아민 계열 물질 중 도파민의 활성 정도가 본 연구 가설의 주의력결핍

과잉행동장애와 같은 신경정신과적 질병의 발병기전의 주요 인자임을 제시한다면, 이를 표적화하는 신약개발의 발판이 될 수 있을 것으로 기대된다.